Inorganic Chemistry

ARTICLE

pubs.acs.org/IC

Azadibenzophospholes: Functional Building Blocks with Pronounced Electron-Acceptor Character

Stefan Durben and Thomas Baumgartner*

Department of Chemistry, University of Calgary, 2500 University Drive NW, Calgary, Alberta T2N 1N4, Canada

Supporting Information

ABSTRACT: A series of azadibenzophospholes with varying location of the nitrogen center has been synthesized and comprehensively characterized. In the context of the study, suitably brominated phenylpyridine precursors were accessed via Suzuki−Miyaura cross-coupling for the first time. Despite being nonfluorescent, X-ray crystallographic studies of two azadibenzophosphole oxides revealed planar conjugated scaffolds with high degree of π−conjugation. The *P*-oxidized species were found to show desirable reversible reduction features that support promising electron-accepting properties of the materials. The presence of the nitrogen as well as phosphorus centers within the scaffold allowed for further functionalization with transition metals, as well as methyl groups that result in altered absorption and redox features for the materials. Subsequent bromination of the scaffold selectively occurred at the exocyclic P-phenyl group, as confirmed via X-ray crystallography. This halogenation allowed for further modification of the system via catalytic cross-coupling with pyridine.

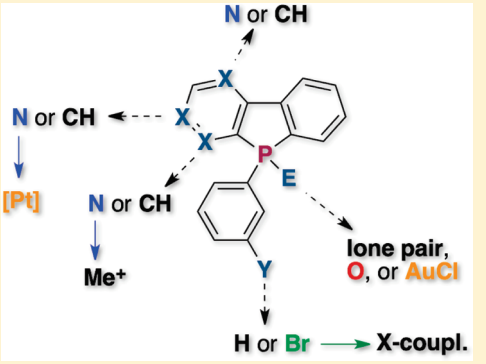

INTRODUCTION

Research in the field of π-conjugated organic materials has for a long time been focused on the development and application of *p*-type semiconductors such as oligoacenes,[1] fused and nonfused oligo- and polythiophenes,[2,3] fluorenes[4] and carbazoles.[5] However, the necessity for accessing *n*-type materials with good processability and electron-conducting features has recently been recognized and thus led to an increased research effort in this area.[6,7] While the array of accessible *p*-type materials is large, the number of suitable *n*-type materials is still limited to date. Moreover, the resulting devices often suffer from an imbalanced charge carrier transport between holes and electrons, limiting the overall performance.[8] To harvest the full potential of molecular electronics, *n*-type materials with high electron mobilities that are similar to the hole mobilities of established *p*-type materials are therefore sought after. An effective strategy toward the generation of *n*-type or ambipolar semiconductors is the functionalization of hydrocarbon scaffolds with fluorine-,[9] cyano-,[10] or phosphine oxide substituents.[11] Furthermore, replacement of CH-groups with electron-withdrawing elements such as boron,[12] or functional groups, such as carbonyls,[6a,10a] or imines[1e,6c,13] has been employed. Even incorporation of oxidized phosphorus centers into the scaffold of conjugated materials has been identified to afford desirable electron-accepting features.[6b,14] All these modifications usually result in stabilized lowest unoccupied molecular orbital (LUMO) energy levels, providing materials that are easily reducible. Many of these materials were also found to function as electron conductors in a device setting. Nitrogen-containing heteroacenes such as **I**,[13a,b] **II**,[13c] and **III**[6c] (Chart 1) are interesting species in this context, as they showcase the transition from *p*-type (in the all hydrocarbon analogues) to *n*-type character upon introduction of electron-poor *N*-heterocycles.

Tetraazapentacene derivative **I** shows a low first reduction potential (E_{red} = −0.79 V, vs Fc/Fc^+) and, in contrast to parent pentacene, pronounced *n*-type behavior in OFET devices.[13a,b] The pyrazinacenes **IIa/b** show low first reduction potentials E_{red} (**IIa**: −0.24 V; **IIb**: −1.20 V, vs Fc/Fc^+), indicating their potential for an application as electron transport materials. Upon introduction of the electron-donating methoxide substituent (**IIb**, R = OMe), the reduction potential is significantly increased (ΔE_{red} = −0.96 V), but notably, still no oxidation is observed up to a potential of E_{ox} = 1 V (vs Fc/Fc^+).[13c] The anthrazoline derivatives **IIIa-d** exhibit reduction potentials comparable to **IIb**, ranging from E_{red} = −1.08 V to −1.15 V (vs Fc/Fc^+), only slightly depending on the nature of the bridge "X".[6c] Furthermore, phosphorus-based systems such as dibenzophosphole oxide **DBPO**,[15] the phosphine oxide substituted examples **IVa/b**[11j] and **V**,[11d] and the fused phosphole oxides **VIa-c**[14c] (Chart 1) have illustrated the applicability of phosphorane moieties in the design of *n*-type materials. Compounds **IVa/b** show reduction waves at E_{red} = −2.26 V (**IVb**) and E_{red} = −2.36 V (**IVa**, vs Fc/Fc^+), respectively. OLEDs using **IVa/b** as hole-blocking and electron-transport materials revealed higher electron mobility for **IVa**, compared to **IVb**.[11j] Compound **V** has been shown to function as a multifunctional material in blue light emitting OLEDs. It simultaneously serves as emitter, electron-transporting, and -injection material.[11d] The annelated phosphole oxides **VIa-c** show consistently low reduction potentials

Received: May 6, 2011
Published: June 15, 2011

Chart 1. Examples of N- and P-Containing Electron-Acceptor (*n*-Type) Organic Conjugated Materials

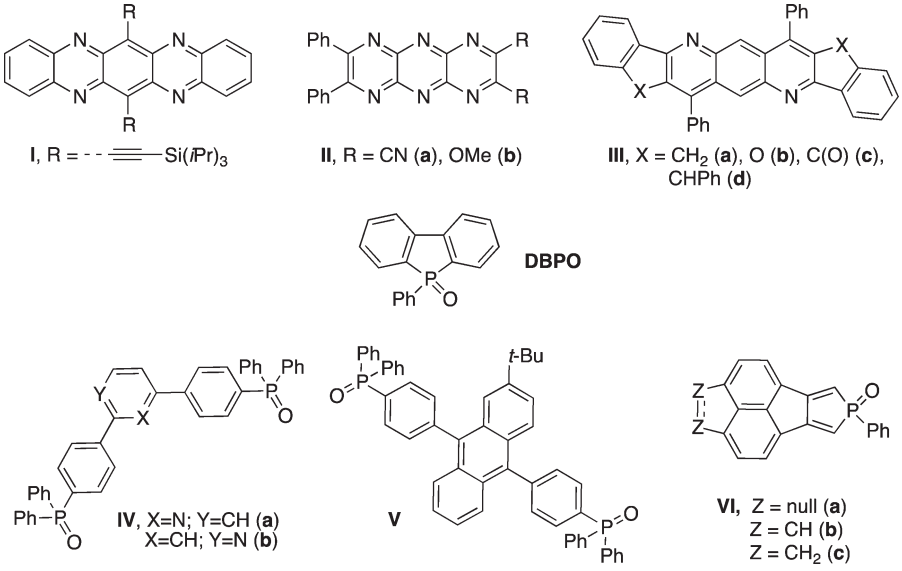

(E_{red} = −1.82 V (**VIa**); −1.62 V (**VIb**); −1.89 V (**VIc**)), indicating potential for an application as electron-transport material.[14c]

In this work, we now report the combination of an electron-poor, *N*-heterocyclic backbone and incorporation of a tunable phosphole moiety to access novel functional electron-acceptor building blocks. The chosen backbone geometry for this fundamental structure−property study is phenylpyridine, offering the possibility to investigate the effect of the position of the imine nitrogen on the materials properties. The combination of the phenylpyridine backbone with the phosphole moiety was expected to have low-lying frontier orbital energy levels and offer the possibility of further chemical functionalization and fine-tuning of the electronic properties via chemical modification of the phosphorus and the imine-nitrogen center, respectively.

EXPERIMENTAL SECTION

General Procedures. Reactions were carried out in dry glassware and under inert atmosphere of purified argon or nitrogen using Schlenk techniques. Solvents were dried over appropriate drying agents and then distilled or used directly from an MBraun solvent purification system. Starting materials were purchased from Aldrich, Alfa Aesar, or Pressure Chemical Co., and used as received. $PhPCl_2$ was distilled prior to use. [Pt(acac)(DMSO)Cl][16] and [Au(tht)Cl][17] were prepared by literature methods. ^{1}H NMR, ^{13}C NMR, and ^{31}P NMR spectra were recorded on Bruker AC200, Bruker DMX-300, or Bruker Avance(-II, -III) 400 spectrometers. Chemical shifts δ were referenced to external 85% H_3PO_4 (^{31}P) or solvent signal (^{1}H, ^{13}C). Elemental analyses were performed at the Department of Chemistry, University of Calgary, on a Perkin-Elmer Model 2400 series II instrument. MALDI/TOF, EI, and ESI mass spectra were recorded on a Bruker Daltonics AutoFlex III, Finnigan SSQ 7000 or Agilent 6520 Q-TOF instrument, respectively. All UV/vis experiments were recorded in dilute dichloromethane solution on a UV−vis−NIR Cary 5000 spectrophotometer. X-ray crystallographic data was measured on a Nonius Kappa CCD diffractometer at 173 K. The structures were solved by direct methods and refined using SHELX. After full-matrix least-squares refinement of the non-hydrogen atoms with anisotropic thermal parameters, the hydrogen atoms were placed in calculated positions using a riding model. Further details on the crystallography can be found in Table 1. Cyclic voltammetry analyses were performed on an Autolab PGSTAT302 instrument, with a polished glassy carbon electrode as the working electrode, a Pt-wire as counter electrode, and an Ag/AgCl/KCl_{3M} reference electrode, using ferrocene/ferrocenium as internal standard. If not otherwise noted, cyclic voltammetry experiments were performed in acetonitrile solution with tetrabutylammonium hexafluorophosphate (0.1 M) as supporting electrolyte. Theoretical calculations have been carried out at the B3LYP/6-31G+(d) level by using the GAUSSIAN 03 suite of programs.[18]

3-Bromo-2-(2-bromophenyl)pyridine 9. 2,3-Dibromopyridine **7** (1.00 g, 4.22 mmol) and 2-bromo-phenylboronic acid **8** (854 mg, 4.22 mmol) were dissolved in tetrahydrofuran (20 mL), aqueous K_2CO_3 (1 M, 15 mL), 5 drops of aqueous KOH (10%) and then degassed. $Pd(PPh_3)_4$ (244 mg, 0.21 mmol) was added and the mixture refluxed for 72 h. After cooling, the phases were separated and the aqueous phase extracted three times with chloroform. The combined organic phases were dried over Na_2SO_4 and concentrated under vacuum. The crude mixture was separated by column chromatography (SiO_2, hexanes/ethylacetate, 2:1, R_f = 0.38), giving 1.22 g (92%) of the title product **9** as colorless oil, which solidified overnight. ^{1}H NMR ($CDCl_3$, 400 MHz): δ = 8.64 (dd, 1 H, ^3J(H,H) = 4.7 Hz, ^4J(H,H) = 1.5 Hz, 6-pyridine), 8.00 (dd, 1 H, ^3J(H,H) = 8.1 Hz, ^4J(H,H) = 1.5 Hz, 4-pyridine), 7.67 (dd, 1 H, ^3J(H,H) = 8.1 Hz, ^4J(H,H) = 1.0 Hz, Ph), 7.42 (td, 1 H, ^3J(H,H) = 7.5 Hz, ^4J(H,H) = 1.2 Hz, Ph), 7.35−7.27 (complex area, 2 H) 7.23 (dd, 1 H; ^3J(H,H) = 8.1 Hz, ^4J(H,H) = 4.7 Hz, 5-pyridine); ^{13}C{^{1}H} NMR ($CDCl_3$, 100.6 MHz): δ = 158.5 (C), 147.8 (CH), 141.0 (C), 140.4 (CH), 132.7 (CH), 130.2 (CH), 130.0 (CH), 127.3 (CH), 124.1 (CH), 122.4 (CH), 121.3 (C) ppm; HRMS (EI, 70 eV): *m*/*z* calcd for $C_{11}H_7Br_2N$: 312.8925 [M^+]; found: 312.8933; elemental analysis calcd (%) for $C_{11}H_7Br_2N$: C 42.21, H 2.25, N 4.48; found: C 42.32, H 2.39, N 4.44.

3-Bromo-4-(2-bromophenyl)pyridine 12. 3-Bromo-4-iodopyridine **11** (1.50 g, 5.3 mmol) and 2-bromophenylboronic acid **8** (1.06 g, 5.3 mmol) were dissolved in tetrahydrofuran (35 mL), aqueous K_2CO_3 (1 M, 25 mL), 5 drops of aqueous KOH (10%), and degassed. $Pd(PPh_3)_4$ (306 mg, 0.27 mmol) was added, and the mixture refluxed for 72 h. After cooling, the phases were separated, and the aqueous phase extracted with chloroform. The combined organic phases were dried with Na_2SO_4 and concentrated under vacuum. The crude mixture was separated by column chromatography (SiO_2, hexanes/ethyl acetate, 4:1), giving 1.49 g (90%) of

dx.doi.org/10.1021/ic200951x |*Inorg. Chem.* 2011, 50, 6823–6836

Table 1. Crystal Data and Structure Refinement for 1b, 4b, and 21

	1b	4b	21
empirical formula	$C_{17}H_{12}NOP$	$C_{17}H_{12}NOP$	$C_{17}H_{11}BrNOP$
formula weight	277.26	277.26	356.14
temperature (K)	173(2)	173(2)	173(2)
wavelength (Å)	0.71073	0.71073	0.71073
crystal system	monoclinic	monoclinic	monoclinic
space group	*P*21/*c*	*P*21/*c*	*C*2/*c*
a (Å)	11.3208(3)	9.9305(7)	26.4755(11)
b (Å)	8.4178(4)	9.5391(4)	8.7326(4)
c (Å)	16.3424(9)	14.1372(9)	13.7296(8)
β (deg)	119.650(8)	92.259(2)	115.3807(26)
volume (Å^3)	1353.49(15)	1338.15(14)	2867.9(3)
Z	4	4	8
density, calcd (Mg/m^3)	1.361	1.376	1.650
abs. coefficient (mm^{-1})	0.501	0.199	2.975
F(000)	576	576	1424
crystal size (mm^3)	0.24 × 0.19 × 0.11	0.12 × 0.08 × 0.03	0.05 × 0.05 × 0.02
θ range (deg)	2.07−27.46	2.58−27.48	1.70−27.55
reflections collected	4654	4658	10809
independent reflections	3064 [*R*(int) = 0.0228]	2992 (*R*(int) = 0.0193)	3282 (*R*(int) = 0.0879)
data/restraints/parameters	3064/0/193	2992/0/181	3282/0/190
GoF on F^2	1.217	1.191	1.105
final *R* indices [$I > 2\sigma(I)$]	R_1 = 0.0506	R_1 = 0.0485	R_1 = 0.0595
	wR_2 = 0.1412	wR_2 = 0.1373	wR_2 = 0.1205
R indices (all data)	R_1 = 0.0592	R_1 = 0.0574	R_1 = 0.0897
	wR_2 = 0.1586	wR_2 = 0.1591	wR_2 = 0.1375

the title product **12** as colorless oil, which solidified overnight. ^{1}H NMR ($CDCl_3$, 400 MHz): δ = 8.82 (s, 1 H, 2-pyridine), 8.57 (d, 1 H, ^3J(H,H) = 4.9 Hz, 6-pyridine), 7.78 (dd, 1 H, ^3J(H,H) = 8.0 Hz, ^4J(H,H) = 1.1 Hz, Ph), 7.40 (td, 1 H, ^3J(H,H) = 7.5 Hz, ^4J(H,H) = 1.2 Hz, Ph), 7.30 (dt, 1 H; ^3J(H,H) = 8.0 Hz, ^4J(H,H) = 1.8 Hz, Ph), 7.20−7.17 (complex area, 2 H); ^{13}C{^{1}H} NMR ($CDCl_3$, 100.6 MHz): δ = 152.2 (CH), 149.4 (C), 148.1 (CH), 139.4 (C), 132.9 (CH), 130.2 (CH), 130.2 (CH), 127.4 (CH), 125.6 (CH), 122.2 (C), 122.0 (C) ppm; HRMS (EI, 70 eV): *m*/*z* calcd for $C_{11}H_7Br_2N$: 312.8925 [M^+]; found: 312.8928; elemental analysis calcd (%) for $C_{11}H_7Br_2N$: C 42.21, H 2.25, N 4.48; found: C 42.57, H 2.22, N 4.37.

3-(2-Bromophenyl)-2-chloropyridine 14. 2-Chloro-3-iodopyridine **13** (1.00 g, 4.2 mmol), 2-bromophenylboronic acid **8** (844 mg, 4.2 mmol), and xantphos (122 mg, 0.21 mmol) were dissolved in tetrahydrofuran (15 mL) and aqueous K_2CO_3 solution (1 M, 12 mL). The biphasic mixture was degassed and subsequently $Pd(PPh_3)_4$ (243 mg, 0.21 mmol) was added. The solution was heated to reflux and stirred for 72 h. After cooling, the phases were separated, and the aqueous phase extracted with chloroform. The combined organic phases were dried with $MgSO_4$ and concentrated under vacuum. The crude mixture was separated by column chromatography (SiO_2, hexanes/ethylacetate, 4:1), giving 876 mg (78%) of the title product **14** (R_f = 0.32) as slightly yellow oil. ^{1}H NMR (CD_2Cl_2, 400 MHz): δ = 8.44 (dd, 1 H, ^3J(H,H) = 4.8 Hz, ^4J(H,H) = 2.0 Hz, 6-pyridine), 7.73 (ddd, 1 H, ^3J(H,H) = 8.0 Hz, ^4J(H,H) = 1.2 Hz, ^5J(H,H) = 0.4 Hz, 6-Ph), 7.63 (dd, 1 H, ^3J(H,H) = 7.5 Hz, ^4J(H,H) = 2.0 Hz, 4-pyridine), 7.43 (td, 1 H, ^3J(H,H) = 7.5 Hz, ^4J(H, H) = 1.2 Hz, Ph), 7.35 (dd, 1 H, ^3J(H,H) = 7.5 Hz, ^3J(H,H) = 4.8 Hz, 5-pyridine), 7.32 (dd, 1 H, ^3J(H,H) = 15.5 Hz, ^4J(H,H) = 1.8 Hz, Ph), 7.31 (ddd, 1 H, ^3J(H,H) = 15.5 Hz, ^4J(H,H) = 1.8 Hz, ^5J(H,H) = 0.4 Hz, 3-Ph); ^{13}C{^{1}H} NMR (CD_2Cl_2, 100.6 MHz): δ = 150.7 (C), 149.8 (CH), 140.4 (CH), 139.1 (C), 136.9 (C), 133.3 (CH), 131.6 (CH), 130.7 (CH), 128.1 (CH), 123.9 (C), 122.9 (CH) ppm; HRMS (EI, 70 eV): *m*/*z* calcd for $C_{11}H_7BrClN$: 268.9430 [M^+]; found: 268.9442.

2-Bromo-3-(2-bromophenyl)pyridine 15. 3-(2-Bromophenyl)-2-chloropyridine **14** (840 mg, 3.13 mmol) was dissolved in PBr_3 (10 mL, ∼106 mmol) and heated to 140 °C for 16 h. The volatiles were removed and fresh PBr_3 (10 mL, ∼106 mmol) was added, and the mixture heated to 140 °C for another 24 h. The volatiles were removed under vacuum, and the resulting mixture neutralized with aqueous Na_2CO_3 solution (sat.). The aqueous phase was extracted three times with chloroform, the combined organic phases dried over Na_2SO_4, and concentrated. The crude mixture was separated by column chromatography (SiO_2, hexanes/ethylacetate, 2:1, R_f = 0.46), giving 836 mg (85%) of the title product **15** as colorless oil, which solidified overnight. ^{1}H NMR (CD_2Cl_2, 400 MHz): δ = 8.40 (dd, 1 H, ^3J(H,H) = 4.8 Hz, ^4J(H,H) = 2.0 Hz, 6-pyridine), 7.71 (ddd, 1 H, ^3J(H,H) = 8.0 Hz, ^4J(H,H) = 1.2 Hz, ^5J(H,H) = 0.4 Hz, Ph), 7.58 (dd, 1 H, ^3J(H,H) = 7.5 Hz, ^4J(H,H) = 2.0 Hz, 4-pyridine), 7.43 (td, 1 H, ^3J(H,H) = 7.5 Hz, ^4J(H,H) = 1.2 Hz, Ph), 7.38 (dd, 1 H, ^3J(H,H) = 7.5 Hz, ^3J(H,H) = 4.8 Hz, 5-pyridine), 7.31−7.27 (complex area, 2 H, Ph); ^{13}C{^{1}H} NMR (CD_2Cl_2, 100.6 MHz): δ = 150.0 (CH), 143.4 (C), 140.5 (C), 139.8 (CH), 139.7 (C), 133.3 (CH), 131.6 (CH), 130.7 (CH), 128.1 (CH), 123.8 (C), 123.2 (CH) ppm; HRMS (EI, 70 eV): *m*/*z* calcd for $C_{11}H_7Br_2N$: 312.8925 [M^+]; found: 312.8924; elemental analysis calcd (%) for $C_{11}H_7Br_2N$: C 42.21, H 2.25, N 4.48; found: C 42.27, H 2.18, N 4.46.

1-Azadibenzophosphole 1a. 3-Bromo-2-(2-bromophenyl)pyridine **9** (313 mg, 1.0 mmol) was dissolved in dry diethyl ether (40 mL), and *t*-BuLi (1.25 mL, 1.6 M in pentane) was added dropwise at −78 °C. The mixture was stirred for 1 h at this temperature, phenyldichlorophosphane (181 mg, 1.0 mmol) was added, and subsequently quickly heated to room temperature (rt). The yellow suspension was concentrated (15 mL), filtered over neutral alumina, and washed with diethyl ether. The filtrate was concentrated, and the

dx.doi.org/10.1021/ic200951x |*Inorg. Chem.* 2011, 50, 6823–6836

yellow crude product was washed twice with cold pentane (10 mL) and dried to give 152 mg (58%) of the title product **1a** as slightly yellow powder. ^{1}H NMR (CD_2Cl_2, 400 MHz): δ = 8.67 (dd, 1 H, ^3J(H,P) = 4.8 Hz, ^4J(H,H) = 1.7 Hz, 2-H), 8.29−8.32 (m, 1 H, 4-H), 8.01 (ddd, 1 H, ^3J(H,H) = 7.6 Hz, ^4J(H,P) = 3.9 Hz, ^4J(H,H) = 1.7 Hz, 3-H), 7.78−7.70 (m, 1 H, Ar), 7.60−7.54 (m, 1 H, Ar), 7.50−7.44 (m, 1 H, Ar), 7.35−7.20 (m, 6 H, Ph and Ar); ^{31}P{^{1}H} NMR (CD_2Cl_2, 162.0 MHz): δ = −16.5; ^{13}C{^{1}H} NMR (CD_2Cl_2, 100.6 MHz): δ = 161.5 (d, J(C,P) = 6.0 Hz, C), 150.5 (s, CH), 143.9 (d, J(C,P) = 1.8 Hz, C), 143.4 (d, J(C,P) = 4.0 Hz, C), 138.5 (d, J(C,P) = 20.1 Hz, CH), 137.5 (d, J(C,P) = 6.5 Hz, C), 135.5 (d, J(C,P) = 18.4 Hz, C), 133.2 (d, J(C,P) = 20.5 Hz, CH), 130.9 (d, J(C,P) = 21.6 Hz, CH), 130.2 (d, J(C,P) = 1.0 Hz, CH), 129.9 (d, J(C,P) = 7.7 Hz, CH), 129.7 (s, CH), 129.4 (d, J(C,P) = 7.8 Hz, CH), 123.5 (s, CH), 122.5 (d, J(C,P) = 5.7 Hz, CH) ppm; HRMS (EI, 70 eV): m/z calcd for $C_{17}H_{12}NP$: 261.0707 [M^+]; found: 261.0659; elemental analysis calcd (%) for $C_{17}H_{12}NP$: C 78.15, H 4.63, N 5.36; found: C 77.97, H 4.82, N 5.27.

1-Azadibenzophosphole oxide 1b. 1-Azadibenzophosphole **1a** (159 mg, 0.61 mmol) was dissolved in chloroform (20 mL) and water (15 mL). H_2O_2 (30%, 1 mL) was added, and the mixture was vigorously stirred for 2 h. The organic phase was separated, the aqueous phase washed twice with chloroform, and the combined organic phases dried over Na_2SO_4 and concentrated. The yellow solid was washed twice with cold pentane (10 mL) and dried to give 160 mg (95%) of the title product **1b** as slightly yellow powder. ^{1}H NMR (CD_2Cl_2, 400 MHz): δ = 8.75 (ddd, 1 H, ^3J(H,H) = 5.0 Hz, ^5J(H,P) = 2.2 Hz, ^4J(H,H) = 1.7 Hz, 2-H), 8.28−8.20 (m, 1 H, Ar), 7.99 (ddd, 1 H, ^3J(H,P) = 9.1 Hz, ^3J(H,H) = 7.5 Hz, ^4J(H,H) = 1.7 Hz, 4-H), 7.78−7.68 (m, 2 H, Ph), 7.67−7.58 (m, 2 H, Ph and Ar), 7.58−7.50 (m, 2 H, Ph), 7.46−7.38 (m, 2 H, Ar), 7.30 (ddd, 1 H, ^3J(H,H) = 7.5 Hz, ^3J(H,H) = 5.0 Hz, ^4J(H,P) = 3.2 Hz, 3-H); ^{31}P{^{1}H} NMR (CD_2Cl_2, 162.0 MHz): δ = 29.7; ^{13}C{^{1}H} NMR (CD_2Cl_2, 100.6 MHz): δ = 160.4 (d, J(C,P) = 24.5 Hz, C), 154.4 (d, J(C,P) = 1.5 Hz, CH), 142.9 (d, J(C,P) = 16.0 Hz, C), 137.8 (d, J(C,P) = 8.3 Hz, CH), 134.5 (d, J(C,P) = 104.2 Hz, C, ipso-Py), 134.3 (d, J(C,P) = 2.3 Hz, CH), 133.0 (d, J(C,P) = 2.9 Hz, CH), 131.8 (d, J(C,P) = 11.5 Hz, CH), 131.5 (d, J(C,P) = 11.0 Hz, CH), 131.0 (d, J(C,P) = 104.9 Hz, C, ipso-Ar), 129.9 (d, J(C,P) = 8.8 Hz, CH), 129.4 (d, J(C,P) = 12.7 Hz, CH) 128.6 (d, J(C,P) = 106.1 Hz, C, ipso-Ar), 124.2 (d, J(C,P) = 8.3 Hz, CH), 123.0 (d, J(C,P) = 10.3 Hz, CH) ppm; HRMS (EI, 70 eV): m/z calcd for $C_{17}H_{12}NOP$: 277.0657 [M^+]; found: 277.0645; elemental analysis calcd (%) for $C_{17}H_{12}NOP$: C 73.64, H 4.36, N 5.05; found: C 73.22, H 4.49, N 5.04.

3-Azadibenzophosphole Oxide 3b. 3-Bromo-4-(2-bromophenyl)pyridine **12** (314 mg, 1.0 mmol) was dissolved in dry diethyl ether (40 mL) and *t*-BuLi (1.25 mL, 1.6 M in pentane) was added dropwise at −78 °C. The mixture was stirred for 1 h at this temperature, phenyldichlorophosphane (184 mg, 1.0 mmol) was added and subsequently quickly heated to rt. The yellow suspension was filtered over neutral alumina and washed with degassed diethyl ether/dichloromethane (1:1). The filtrate was concentrated, and the yellow crude product **3a** was taken up in chloroform (25 mL). To this water (15 mL) and H_2O_2 (30%, 1 mL) were added and the emulsion vigorously stirred for 2 h. The organic phase was separated, the aqueous phase washed twice with chloroform and the combined organic phases dried over Na_2SO_4 and concentrated. The yellow solid was washed twice with cold pentane (10 mL) and dried to give 192 mg (69%) of the title product **3b** as slightly yellow powder. ^{1}H NMR ($CDCl_3$, 400 MHz): δ = 8.91 (dd, 1 H, ^3J(H,P) = 4.4 Hz, ^5J(H,H) = 1.0 Hz, 4-H), 8.82 (dd, 1 H, ^3J(H,H) = 5.2 Hz, ^5J(H,P) = 2.4 Hz, 2-H), 7.92 (br. dd, 1 H, J(H,H) = 7.7 Hz, J(H,P) = 2.9 Hz, Ar), 7.82−7.75 (m, 1H, Ar), 7.72 (ddd, 1 H, ^3J(H,H) = 5.2 Hz, ^4J(H,P) = 2.3 Hz, ^5J(H,H) = 1.0 Hz, 1-H), 7.70−7.62 (m, 3 H, *o*-Ph and Ar), 7.59−7.51 (m, 2 H, *p*-Ph and Ar), 7.46−7.39 (m, 2 H, *m*-phenyl); ^{31}P{^{1}H} NMR ($CDCl_3$, 162.0 MHz): δ = 34.0; ^{13}C{^{1}H} NMR ($CDCl_3$, 100.6 MHz): δ = 154.2 (d, J(C,P) = 0.9 Hz, CH), 150.8 (d, J(C,P) = 10.6 Hz, CH), 149.5 (d, J(C,P) = 20.0 Hz, C), 139.3 (d, J(C,P) = 21.0 Hz, C), 133.7 (d, J(C,P) = 2.0 Hz, CH), 133.5 (d, J(C,P) = 106.9 Hz, C), 132.7 (d, J(C,P) = 2.9 Hz, CH), 131.9 (d, J(C,P) = 11.1 Hz, CH), 131.0 (d, J(C,P) = 11.1 Hz, CH), 130.2 (d, J(C,P) = 9.8 Hz, CH), 129.5 (d, J(C,P) = 106.1 Hz, C), 129.0 (d, J(C,P) = 13.0 Hz, CH) 128.1 (d, J(C,P) = 103.7 Hz, C), 122.5 (d, J(C,P) = 9.7 Hz, CH), 115.8 (d, J(C,P) = 7.8 Hz, CH) ppm; HRMS (EI, 70 eV): m/z calcd for $C_{17}H_{12}NOP$: 277.0657 [M^+]; found: 277.0652; elemental analysis calcd (%) for $C_{17}H_{12}NOP$: C 73.64, H 4.36, N 5.05; found: C 73.29, H 4.57, N 4.94.

NMR-Data for Phosphole 3a. ^{1}H NMR (CD_2Cl_2, 400 MHz): δ = 8.88 (ps. t, 1 H, J = 1.1 Hz, Py), 8.66 (d, 1 H, J = 5.2 Hz, Py), 8.05−7.99 (m, 1 H, Ar), 7.82−7.77 (m, 1 H, Ar), 7.77−7.72 (m, 1 H, Ar), 7.56−7.49 (m, 1 H, Ar), 7.48−7.42 (m, 1 H, Ar), 7.31−7.19 (m, 5 H, Ph); ^{31}P{^{1}H} NMR (CD_2Cl_2, 400 MHz): δ = −12.3 ppm.

4-Azadibenzophosphole 4a. 2-Bromo-3-(2-bromophenyl)pyridine **15** (627 mg, 2.0 mmol) was dissolved in dry diethyl ether (85 mL) and *t*-BuLi (2.50 mL, 1.6 M in pentane) was added dropwise at −78 °C. The mixture was stirred for 1 h at this temperature, phenyldichlorophosphane (359 mg, 2.0 mmol) was added and subsequently quickly heated to rt. The yellow suspension was concentrated (35 mL), filtered over neutral alumina, and washed with diethyl ether. The filtrate was concentrated, and the yellow crude product was washed twice with 20 mL of cold pentane and dried to give 361 mg (69%) of the title product **4a** as slightly yellow powder. ^{1}H NMR (CD_2Cl_2, 400 MHz): δ = 8.61 (dd, 1 H, ^3J(H,H) = 4.8 Hz, ^4J(H,H) = 1.5 Hz, 3-H), 8.15 (ps. dt, 1 H, J = 7.9 Hz, J = 1.6 Hz, 1-H), 7.98 (br. d, 1 H, J = 7.8 Hz, Ar), 7.85−7.78 (m, 1 H, Ar), 7.58−7.51 (m, 1 H, Ar), 7.53−7.37 (m, 3 H, Ph and Ar), 7.34 (dd, 1 H, ^3J(H,H) = 7.9 Hz, ^3J(H,H) = 4.8 Hz, 2-H), 7.32−7.24 (m, 3 H, Ph); ^{31}P{^{1}H} NMR (CD_2Cl_2, 162.0 MHz): δ = −14.8; ^{13}C{^{1}H} NMR (CD_2Cl_2, 100.6 MHz): δ = 169.4 (d, J(C,P) = 12.1 Hz), 150.0 (d, J(C,P) = 11.3 Hz), 141.9 (s), 141.3 (d, J(C,P) = 3.5 Hz), 138.3 (d, J(C,P) = 9.1 Hz), 135.0 (d, J(C,P) = 19.3 Hz), 133.0 (d, J(C,P) = 19.0 Hz, C), 131.4 (d, J(C,P) = 21.4 Hz), 129.8 (br. s), 129.7 (s), 129.3 (d, J(C,P) = 7.4 Hz), 128.9 (d, J(C,P) = 7.4 Hz, CH), 128.6 (s), 123.1 (s), 122.6 (s) ppm; HRMS (EI, 70 eV): m/z calcd for $C_{17}H_{12}NP$: 261.0707 [M^+]; found: 261.0714; elemental analysis calcd (%) for $C_{17}H_{12}NP$: C 78.15, H 4.63, N 5.36; found: C 78.45, H 4.83, N 5.27.

4-Azadibenzophosphole Oxide 4b. 4-Azadibenzophosphole **4a** (189 mg, 0.72 mmol) was dissolved in chloroform (20 mL) and water (15 mL). H_2O_2 (30%, 1 mL) was added, and the mixture was vigorously stirred for 2 h. The organic phase was separated, the aqueous phase washed twice with chloroform, and the combined organic phases dried over Na_2SO_4 and concentrated. The yellow solid was washed twice with cold pentane (10 mL) and dried to give 179 mg (89%) of the title product as slightly yellow powder. ^{1}H NMR (CD_2Cl_2, 400 MHz): δ = 8.65 (dd, 1 H, ^3J(H,H) = 4.8 Hz, ^4J(H,H) = 1.4 Hz, 3-H), 8.10 (ddd, 1 H, ^3J(H,H) = 8.0 Hz, ^3J(H,P) = 4.1 Hz, ^4J(H,H) = 1.4 Hz, 1-H), 7.90−7.85 (m, 1 H, Ar), 7.81−7.75 (m, 1 H, Ar), 7.70−7.61 (m, 3 H, Ph and Ar), 7.57−7.47 (m, 2 H, Ph and Ar), 7.45 (ddd, 1 H, ^3J(H,H) = 8.0 Hz, ^3J(H,H) = 4.8 Hz, ^5J(H,P) = 1.1 Hz, 2-H), 7.44−7.38 (m, 2 H, Ph); ^{31}P{^{1}H} NMR (CD_2Cl_2, 162.0 MHz): δ = 25.1; ^{13}C{^{1}H} NMR (CD_2Cl_2, 100.6 MHz): δ = 158.1 (d, J(C,P) = 132.3 Hz, C), 151.8 (d, J(C,P) = 17.0 Hz, CH), 139.9 (d, J(C,P) = 16.9 Hz, C), 137.5 (d, J(C,P) = 35.3 Hz, C), 134.3 (d, J(C,P) = 1.8 Hz, CH), 133.0 (d, J(C,P) = 2.9 Hz, CH), 131.9 (d, J(C,P) = 106.1 Hz, C), 131.7 (d, J(C,P) = 10.8 Hz, CH), 130.8 (d, J(C,P) = 10.9 Hz, CH), 130.6 (d, J(C,P) = 9.1 Hz, CH), 130.2 (d, J(C,P) = 101.2 Hz, C), 129.4 (d, J(C,P) = 12.6 Hz, CH), 128.9 (d, J(C,P) = 8.4 Hz, CH), 126.9 (d, J(C,P) = 2.7 Hz, CH), 122.6 (d, J(C,P) = 8.3 Hz, CH) ppm; elemental analysis calcd (%) for $C_{17}H_{12}NOP$: C 73.64, H 4.36, N 5.05; found: C 73.69, H 4.48, N 4.93.

Pt-Complex 17. To a solution of 3-azadibenzophosphole oxide **3b** (62 mg, 0.22 mmol) in ethanol (5 mL), a solution of potassium tetrachloroplatinate(II) (46 mg, 0.11 mmol) in water (5 mL) was added at rt. The yellow solution was stirred for 18 h at 50 °C, during which a white precipitate formed. After cooling, the white solid was filtered off, washed with water and dried under vacuum to give 58 mg (62%) of the title product **17.** ^{1}H NMR ($CDCl_3$, 400 MHz): δ = 9.12 (d, 1 H,

^3J(H−P) = 5.8 Hz, 4-H), 9.05 (dd, 1 H, ^3J(H−H) = 6.2 Hz, ^5J(H−P) = 1.6 Hz, 2-H), 7.95 (dd, 1 H, J = 7.7 Hz, J = 2.9 Hz, Ar), 7.82 (dd, J = 7.3 Hz, J = 10.1 Hz, Ar), 7.73 (m, 1 H, Ar), 7.70−7.54 (m, 4 H, Ar and Ph), 7.50−7.41 (m, 1 H, *m*-Ph); $^{31}P\{^1H\}$ NMR ($CDCl_3$, 162.0 MHz): δ = 32.1; ^{195}Pt NMR ($CDCl_3$, 86.0 MHz): δ = −312.2 ppm; The low solubility in common organic solvents precluded ^{13}C NMR spectroscopy in solution; HRMS (ESI): m/z calcd for $C_{34}H_{24}Cl_2N_2NaO_2P_2Pt$: 843.02217 [$M^+$ + Na]; found: 843.02419; elemental analysis calcd (%) for $C_{34}H_{24}Cl_2N_2O_2P_2Pt$: C 49.77, H 2.82, N 3.18 ; found: C 48.78, H 2.73, N 3.10.

4-Azadibenzophosphole-methyltriflate Adduct 19. To a solution of 4-azadibenzophosphole **4a** (137 mg, 0.52 mmol) in dichloromethane (15 mL), a solution of MeOTf (86 mg, 0.52 mmol) in dichloromethane (10 mL) was dropwise added at 0 °C. The volatiles were removed, and the yellow powder washed three times with cold pentane to give 201 mg (90%) of the title product **19** as yellow solid. ^1H NMR (CD_2Cl_2, 400 MHz): δ = 9.00 (dd, 1 H, ^3J(H,H) = 5.8 Hz, ^4J(H,H) = 2.8 Hz, 3-H), 8.92 (br. d, 1 H, J = 8.1 Hz, 1-H), 8.22 (dd, 1 H, J = 7.9 Hz, Ar), 8.17−8.10 (m, 1 H, 2-H), 7.81−7.75 (m, 1 H, Ar), 7.73 (td, 1 H, ^3J(H,H) = 7.6 Hz, ^4J(H,H) = 1.2 Hz, Ar), 7.66−7.59 (m, 1 H, Ar) 7.55−7.48 (m, 1 H, Ph), 7.43−7.36 (m, 2 H, Ph), 7.35−7.27 (m, 2 H, Ph), 4.32 (s, 3 H, CH_3); $^{31}P\{^1H\}$ NMR (CD_2Cl_2, 162.0 MHz): δ = −10.4; $^{13}C\{^1H\}$ NMR (CD_2Cl_2, 100.6 MHz): δ = 164.1 (d, J(C,P) = 18.4 Hz), 145.8 (s), 144.7 (d, J(C,P) = 4.5 Hz), 139.8 (d, J(C,P) = 1.2 Hz), 138.4 (s), 136.6 (s), 135.5 (d, J(C,P) = 22.7 Hz), 133.0 (d, J(C,P) = 1.4 Hz), 132.2 (d, J(C,P) = 8.8 Hz), 131.3 (s), 131.0 (d, J(C,P) = 23.8 Hz), 130.7 (d, J(C,P) = 9.5 Hz), 128.5 (d, J(C,P) = 1.1 Hz), 126.0 (d, J(C,P) = 15.2 Hz), 124.5 (s), 121.4 (q, ^1J(C−F) = 320.8 Hz), 48.9 (d, ^3J(C,P) = 10.0 Hz) ppm; elemental analysis calcd (%) for $C_{19}H_{15}F_3NO_3PS$: C 53.65, H 3.55, N 3.29 ; found: C 53.88, H 3.50, N 3.22.

4-Azadibenzophosphole-methyltriflate Adduct Gold Chloride Complex 20. To a solution of 4-azadibenzophosphole-methyltriflate adduct **19** (190 mg, 0.45 mmol) in dichloromethane (20 mL), [Au(tht)Cl] (160 mg, 0.5 mmol) was added, and the solution stirred for 16 h at rt. All volatiles were removed under vacuum, and the crude product recrystallized from hot ethanol to give 160 mg (54%) of the title product **20** as yellow needles. ^1H NMR (CD_2Cl_2, 400 MHz): δ = 9.13−9.01 (m, 2 H, Py), 8.36 (br. dd, 1 H, ^3J(H−H) = 6.1 Hz, ^3J(H−H) = 7.2 Hz, 2-H), 8.27 (dd, 1 H, J = 7.9 Hz, J = 2.5 Hz, Ar), 7.94−7.81 (m, 2 H, Ar), 7.80−7.62 (complex area, 4 H, Ar), 7.61−7.52 (m, 2 H, Ar), 4.45 (s, 3 H, CH_3); $^{31}P\{^1H\}$ NMR (CD_2Cl_2, 162.0 MHz): δ = 25.8; $^{13}C\{^1H\}$ NMR (CD_2Cl_2, 100.6 MHz): δ = 150.5 (d, ^1J(C−P) = 60.6 Hz, ipso-Py), 148.2 (s, Py), 144.3 (d, J(C−P) = 14.2 Hz, Py), 138.2 (d, J(C−P) = 4.0 Hz, Ar), 137.2 (d, J(C−P) = 6.7 Hz, Ar), 135.4 (d, J(C−P) = 16.8 Hz, Ar), 135.4 (d, J(C−P) = 2.8 Hz, Ar), 134.4 (d, J(C−P) = 2.0 Hz, Ar), 133.0 (d, J(C−P) = 13.1 Hz, Ar), 131.6 (s, Ar), 131.5 (d, J(C−P) = 23.8 Hz, Ar), 130.8 (d, J(C−P) = 13.4 Hz, Ar), 129.8 (d, ^1J(C−P) = 67.8, ipso-Ar), 124.8 (d, J(C−P) = 6.2 Hz, Ar), 120.6 (q, ^1J(C−F) = 324.2 Hz, CF_3), 119.0 (d, ^1J(C−P) = 59.8 Hz, ipso-Ar), 48.4 (d, ^3J(C−P) = 7.8 Hz, CH_3) ppm; elemental analysis calcd (%) for $C_{19}H_{15}F_3NO_3PSAuCl$: C 34.69, H 2.30, N 2.13; found: C 35.01, H 2.31, N 1.97.

Brominated 4-Azadibenzophosphole 21. To a solution of 4-azadibenzophosphole oxide **4b** (275 mg; 0.99 mmol) in trifluoroacetic acid (25 mL) and sulfuric acid (conc., 2.5 mL), *N*-bromosuccinimide (282 mg, 1.58 mmol) was added in eight portions over 8 h at 0 °C, and the mixture stirred overnight in the dark. The solution was then poured into ice water and neutralized with $NaHCO_3$ solution. The aqueous phase was extracted three times with chloroform, the combined organic phases dried over Na_2SO_4 and concentrated under vacuum. The crude mixture was separated by column chromatography (SiO_2, chloroform/ethyl acetate, 1:1) to give 113 mg (32%) of the product **21** as white powder. ^1H NMR (CD_2Cl_2, 400 MHz): δ = 8.67 (dd, 1 H, ^3J(H−H) = 4.8 Hz, ^4J(H−H) = 1.4 Hz, 3-H), 8.11 (ddd, 1 H, ^3J(H−H) = 8.0 Hz, ^4J(H−P) = 4.2 Hz, ^4J(H−H) = 1.4 Hz, 1-H), 7.88 (br. dd, 1 H, J = 7.7 Hz, J = 3.4 Hz, Ar), 7.82−7.62 (m, 4 H, Ar), 7.62−7.55 (m, 1 H, Ar), 7.55−7.49 (m, 1 H, Ar), 7.47 (ddd, 1 H, ^3J(H−H) = 8.0 Hz, ^3J(H−H) = 4.8 Hz, ^5J(H−P) = 2.2 Hz, 2-H) $^{31}P\{^1H\}$ NMR (CD_2Cl_2, 162 MHz): δ = 23.6; $^{13}C\{^1H\}$ NMR (CD_2Cl_2, 100.6 MHz): δ = 157.4 (d, ^1J(C−P) = 133.7 Hz, C, *ipso*-Py), 152.0 (d, J(C−P) = 17.2 Hz, CH), 139.9 (d, J(C−P) = 17.3 Hz, C), 137.6 (d, J(C−P) = 36.1 Hz, C), 136.1 (d, J(C−P) = 2.7 Hz, CH), 134.7 (d, J(C−P) = 2.0 Hz, CH), 134.3 (d, J(C−P) = 11.7 Hz, CH), 133.0 (d, J(C−P) = 100.0 Hz, C, *ipso*-Ar), 131.2 (d, J(C−P) = 107.4 Hz, C, *ipso*-Ar), 131.1 (d, J(C−P) = 12.5 Hz, CH), 131.0 (d, J(C−P) = 10.6 Hz, CH), 130.8 (d, J(C−P) = 9.2 Hz, CH), 130.4 (d, J(C−P) = 10.3 Hz, CH), 129.1 (d, J(C−P) = 8.6 Hz, CH), 127.2 (d, J(C−P) = 2.7 Hz, CH), 123.7 (d, J(C−P) = 16.0 Hz, C), 122.7 (d, J(C−P) = 8.4 Hz, CH) ppm; HRMS (EI, 70 eV): m/z calcd for $C_{17}H_{11}BrNOP$: 354.9762 [M^+]; found: 354.9757.

Scheme 1. Targeted Azadibenzophospholes and General Synthetic Strategy toward Dithienophospholes

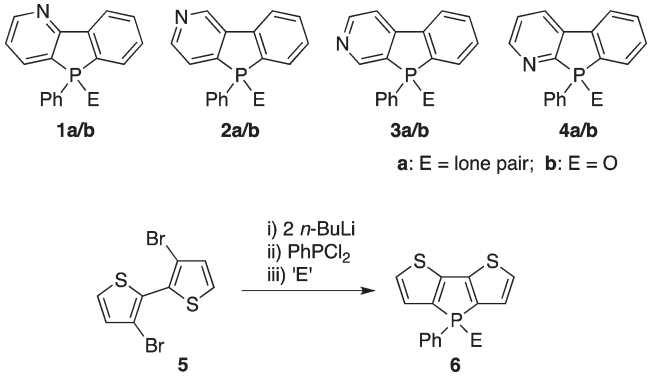

Pyridine-Coupled 4-Azadibenzophosphole 23. A degassed solution of brominated 4-azadibenzophosphole **21** (68 mg, 0.19 mmol), 2-(tributylstannyl)pyridine **22** (105 mg, 0.29 mmol) and [$Pd(PPh_3)_4$] (11 mg, 0.01 mmol) in toluene (5 mL) was refluxed for 48 h. After cooling, chloroform (15 mL) and NH_4Cl-solution (sat., 15 mL) was added. The phases were separated, and the aqueous phase was extracted with chloroform (3 × 10 mL). The organic phases were combined, dried over Na_2SO_4, and concentrated. The orange greasy crude product was separated by column chromatography (SiO_2, chloroform/ethyl acetate, 1:1 + 3% ethanol) to give 52 mg (76%) of the title product **23** as a colorless solid. ^1H NMR (CD_2Cl_2, 400 MHz): δ = 8.66 (dd, 1 H, ^3J(H−H) = 4.8 Hz, ^4J(H−H) = 1.4 Hz, 3-H), 8.65−8.59 (m, 1 H, 6-Pyridyl), 8.36 (br. d, 1 H, J = 13.4 Hz, Ar), 8.25−8.16 (m, 1 H, Ar), 8.12 (ddd, 1 H, ^3J(H−H) = 8.0 Hz, ^4J(H−P) = 4.1 Hz, ^3J(H−H) = 1.4 Hz, 1-H), 7.89 (br. dd, 1 H, J = 7.7 Hz, J = 3.3 Hz, Ar), 7.86−7.79 (m, 1 H, Ar), 7.79−7.64 (complex area, 3 H, Ar), 7.64−7.55 (m, 1 H, Ar), 7.55−7.48 (complex area, 2 H, Ar), 7.46 (ddd, 1 H, ^3J(H−H) = 8.0 Hz, ^3J(H−H) = 4.8 Hz, ^5J(H−P) = 2.1 Hz, 2-H), 7.25 (ddd, 1 H, J = 6.5 Hz, J = 4.8 Hz, J = 2.2 Hz, Ar); $^{31}P\{^1H\}$ NMR (CD_2Cl_2, 162 MHz): δ = 25.2; $^{13}C\{^1H\}$ NMR (CD_2Cl_2, 100.6 MHz): δ = 158.0 (d, J(C−P) = 132.6 Hz, C, *ipso*-Ar), 156.4 (s, C, 2-Pyridyl), 151.9 (d, J(C−P) = 17.1 Hz, CH, Ar), 150.3 (s, CH, Pyridyl), 140.7 (d, J(C−P) = 12.4 Hz, C, Ar), 139.9 (d, J(C−P) = 16.9 Hz, C, Ar), 137.6 (d, J(C−P) = 35.2 Hz, C, Ar), 137.4 (s, CH, Pyridyl), 134.4 (d, J(C−P) = 1.9 Hz, CH, Ar), 131.9 (d, J(C−P) = 11.3 Hz, CH, Ar), 131.9 (d, J(C−P) = 106.3 Hz, C, *ipso*-Ar), 131.5 (d, J(C−P) = 2.8 Hz, CH, Ar), 130.9 (d, J(C−P) = 10.9 Hz, CH, Ar), 130.7 (d, J(C−P) = 11.2 Hz, CH, Ar), 130.7 (d, J(C−P) = 103.1 Hz, C, *ipso*-Ar), 130.2 (d, J(C−P) = 11.2 Hz, CH, Ar), 129.8 (d, J(C−P) = 13.1 Hz, CH, Ar), 129.0 (d, J(C−P) = 8.5 Hz, CH, Ar) 127.0 (d, J(C−P) = 2.5 Hz, CH, Ar), 123.3 (s, CH, Pyridyl), 122.7 (d, J(C−P) = 8.2 Hz, CH, Ar), 121.1 (s, CH, Pyridyl) ppm; HRMS (EI, 70 eV): m/z calcd for $C_{22}H_{15}N_2OP$: 354.0922 [M^+]; found: 354.0914.

dx.doi.org/10.1021/ic200951x |*Inorg. Chem.* 2011, 50, 6823–6836

Scheme 2. Synthesis of the Dibrominated Phenylpyridine Precursors 9, 12, and 15

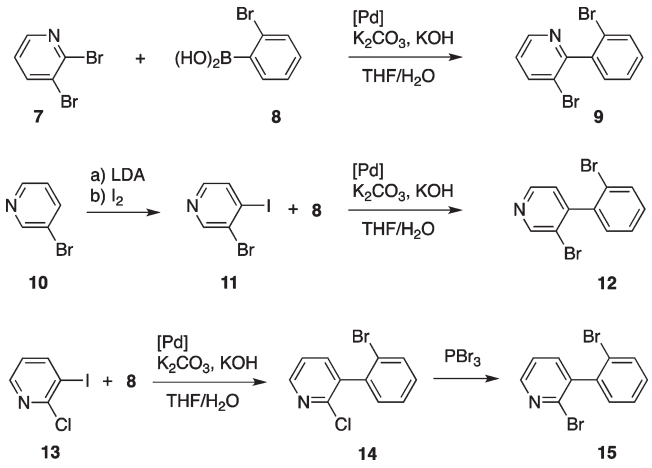

RESULTS AND DISCUSSION

1. Phenylpyridine Starting Materials. *Syntheses.* Our targeted synthetic approach toward the azadibenzophospholes **1**−**4** followed a strategy analogous to that toward the dithieno[3,2-*b*:2′,3′-*d*]phosphole **6**[19] and related systems[20] that we have been systematically investigating in recent years (Scheme 1).

Consequently, access to the corresponding dihalogenated phenylpyridine precursors had to be verified first. The synthesis of the starting material **9** for 1-azadibenzophosphole **1** proved to be facile, starting from commercially available 2,3-dibromopyridine **7** (Scheme 2). Dibromopyridine **7** was cross-coupled to 2-bromophenylboronic acid **8** to give 3-bromo-2-(2-bromophenyl)pyridine **9** in very good yield (92%) as colorless oil, which solidified overnight. Consistent ^{1}H and ^{13}C NMR data as well as MS and CHN analysis supported the successful formation of **9**. The preparation of the corresponding precursor for 2-azadibenzophospholes **2** proved to be challenging and even after several different synthetic attempts, the precursor could not be obtained. By contrast, precursor **12** for the 3-azadibenzophospholes **3** was obtained via a facile approach starting from commercially available 3-bromopyridine **10** (Scheme 2), which was converted to 3-bromo-4-iodopyridine **11** according to a known procedure.[21] Subsequently, Suzuki−Miyaura coupling of **11** with boronic acid **8** gave 3-bromo-4-(2-bromophenyl)pyridine **12** in excellent yield (90%). In addition to consistent NMR-, MS- and CHN-analysis, the identity of **12** was confirmed by single crystal X-ray crystallography (see Supporting Information). The synthesis of the precursor for 4-azadibenzophospholes **4** was achieved using 2-chloro-3-iodopyridine **13**, which was converted to the 3-(2-bromophenyl)-2-chloropyridine **14** via the established Suzuki−Miyaura cross-coupling protocol (Scheme 2).[22] Subsequent treatment with neat tribromophosphane (PBr_3) at elevated temperature (140 °C) for 24 h yielded the 2-bromo-3-(2-bromophenyl)pyridine **15** in good isolated yield (85%) as a colorless solid and single crystals, suitable for X-ray crystallography (see Supporting Information for details).

Photophysics and Electrochemistry. The UV/vis spectra of the dibromo(phenylpyridine)s **9**, **12**, and **15** (see Supporting Information) were measured in dilute dichloromethane (DCM) solution and are summarized in Table 2. All three phenylpyridines show similar absorption features with absorption maxima in the UV range of the optical spectrum (**9**: λ_{max} = 271 nm; **12**: λ_{max} = 269 nm; **15**: λ_{max} = 268 nm). The molar absorptivity rises in the order **12** < **9** < **15**, potentially because of some planarization via Br−H (**9**, **12**, **15**) and/or Br−N (**9**) interactions in solution, which seem to be increasing in strength in the same order (**9**: ε_{max} = 4080 L mol^{-1} cm^{-1}; **12**: ε_{max} = 3240 L mol^{-1} cm^{-1}; **15**: ε_{max} = 5290 L mol^{-1} cm^{-1}). Compounds **9** and **15** exhibit shoulders at 279 and 262 nm, respectively, whereas in **12**, only the low energy transition at 279 nm is observed. The electrochemical properties (Table 2) of dibromo(phenylpyridine)s **9**, **12**, and **15** were studied by means of cyclic voltammetry (CV) in acetonitrile solution with tetrabutylammonium hexafluorophosphate ([NBu_4][PF_6]) as supporting electrolyte, and Fc/Fc^{+} as internal reference (see Supporting Information for details). All three compounds show irreversible reductions at high potentials (**9**: $E_{red,peak}$ = −2.75 V, −2.90 V; **12**: $E_{red,peak}$ = −2.72 V; **15**: $E_{red,peak}$ = −2.82 V) and two irreversible oxidations (**9**: $E_{ox,peak}$ = 0.71 V, 0.94 V; **12**: $E_{ox,peak}$ = 0.78 V, 1.00 V; **15**: $E_{ox,peak}$ = 0.75 V, 0.98 V). Compound **12** also exhibits an additional quasireversible reduction at $E_{red,1/2}$ = −2.89 V, which overlaps with the irreversible reduction.

2. Azadibenzophospholes and Azadibenzophosphole Oxides. *Syntheses and Structures.* With the dibromo(phenylpyridine)s **9**, **12**, and **15** in hand, we then proceeded to synthesize the corresponding azadibenzophospholes **1a**, **3a**, and **4a**. The best results were observed with the use of *t*-BuLi as metalating reagent, diethyl ether as solvent, −78 °C as temperature during the metalation reaction, and 1 h reaction time for metalation. The synthesis of the azadibenzophospholes and corresponding phosphole oxides **1a**/**b**, **3a**/**b**, and **4a**/**b** is outlined in Scheme 3.

Note that all azadibenzophospholes exhibit an asymmetric backbone structure, making the phosphorus atom a stereocenter. Since the reaction conditions did not entail any stereospecific reagents or additives, the products **1a**,**b**, **3a**,**b** and **4a**,**b** were obtained as racemic mixtures (vide infra). 1-Azadibenzophosphole **1a** and 4-azadibenzophosphole **4a** were cleanly formed under the reaction conditions, next to minor amounts of the corresponding oxidized phosphole species **1b** and **4b**. The trivalent species could, however, be isolated analytically pure as slightly yellow powders in moderate yields after workup (**1a**: 58%; **4a**: 69%). The phosphole oxides are formed in the presence of traces of oxygen during workup and show significantly increased polarity over their trivalent congeners because of the generally very polar nature of the P═O bond. Since the backbones of the trivalent **1a** and **4a** exhibit only moderately polar character overall, filtration over alumina with Et_2O efficiently separates the trivalent phospholes from the corresponding oxides. In the case of 3-azadibenzophosphole **3a**, however, the position of the electronegative nitrogen atom evidently makes the scaffold of the trivalent form considerably more polar, and the difference in polarity between phosphole **3a** and phosphole oxide **3b** appears much less pronounced than in the other congeners. Consequently, phosphole **3a** and the corresponding oxide **3b** (∼10%) could not be separated by column chromatography, or by crystallization from various solvents.

The successful formation of the phospholes **1a**, **3a**, and **4a** was supported by multinuclear NMR spectroscopy; ^{1}H NMR analysis indicated the expected additional signals for the *P*-phenyl substituent. It is interesting to note that all resonances of the *P*-phenyl group in compounds **1a** and **3a** fall together in one broad

dx.doi.org/10.1021/ic200951x |*Inorg. Chem.* 2011, 50, 6823–6836

Table 2. Photophysical and Electrochemical Data for 9, 12, and 15

Compd	λ_{abs} [a] [nm]	ε_{max} [a] [L mol^{-1} cm^{-1}]	$E_{red,peak}$ [b] [V]	$E_{red,1/2}$ [c] [V]	$E_{ox,peak}$ [d] [V]
9	271	4080	−2.75/-2.90		0.71/0.94
12	269	3240	−2.72	−2.89	0.78/1.00
15	268	5290	−2.82		0.75/0.98

[a] UV/vis absorption maxima in CH_2Cl_2. [b] Irreversible reduction peak potentials vs Fc/Fc^+. [c] Quasireversible reduction half-step potential vs Fc/Fc^+. [d] Irreversible oxidation peak potentials vs Fc/Fc^+.

Scheme 3. Synthesis of Azadibenzophospholes 1a, 3a, and 4a and the Corresponding Oxides 1b, 3b, and 4b

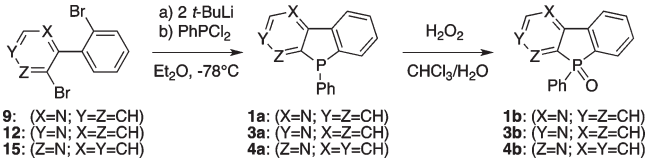

multiplet (δ ^{1}H = 7.35−7.20 ppm), while the resonances for the *P*-phenyl substituent in 4-azadibenzophosphole **4a** split into two groups (δ ^{1}H = 7.33−7.23 ppm [3 H] and 7.44−7.38 ppm [2 H]), probably because of some through-space *N*−*H* interactions of the *o*-hydrogens on the phenyl-ring with the nitrogen in the backbone. Furthermore, the appearance of characteristic ^{31}P NMR resonances indicated the presence of trivalent azadibenzophosphole species (δ ^{31}P = −16.5 (**1a**); −12.3 (**3a**); −14.8 (**4a**) ppm). All ^{31}P NMR signals are shifted upfield relative to dibenzophosphole (δ ^{31}P = −11.7 ppm)[23] and downfield relative to dithienophosphole **6** (E = lone pair; δ ^{31}P = −21.5 ppm).[19a,b]

The oxidation to the corresponding phosphole oxides, according to the established procedure,[19a,b] proceeded cleanly in excellent isolated yields for **1b** (95%) and **4b** (89%). Phosphole oxide **3b** was cleanly obtained from **15** in 69% isolated yield over two steps. The oxidation of the phosphorus centers resulted in significant downfield shifts of the ^{31}P NMR resonances (δ ^{31}P = 29.7 (**1b**); 34.0 (**3b**); 25.1 (**4b**) ppm), comparable to that of dibenzophosphole oxide **DBPO** (δ ^{31}P = 31.4 ppm).[24] In the case of **1b** and **4b**, the successful formation was furthermore confirmed by single-crystal X-ray crystallography (Figures 1 and 2; Table 1). For both compounds, single-crystals could be obtained from a concentrated ethanol solution upon evaporation of the solvent at room temperature. The structure of **1b** showcases a planar backbone with only small C−C bond-length alternation. Compound **1b** exhibits endo- and exocyclic P−C bonds of essentially equal length (1.799(2)−1.809(2) Å), comparable to those observed in dibenzophosphole oxide **DBPO** (1.798(3)−1.801(3) Å).[25] The P−O distance in **1b** (1.4850(16) Å) correlates well to the analogous bond length in **DBPO** (1.475(2) Å). Similarly, the bond angles around the phosphorus atom are in good agreement with those observed in **DBPO**.[25] In the packing motif, close π-stacking interactions (3.35 Å) are observed between inversion-related pairs of enantiomers.

The π−overlap between the molecules is small; only C3, N1, C12, and C13 of the respective molecules are in the overlapping region. No close face-to-face interactions between the phenyl-substituents are observed. Similar to the structure of **1b**, compound **4b** features a planar backbone with little C−C bond-length alternation, which is an expected result for 6π-electron *N*-hetero- and carbocycles. Compound **4b** also exhibits equally long endo- and exocyclic P−C bonds (1.800(2)−1.809(2) Å), comparable to

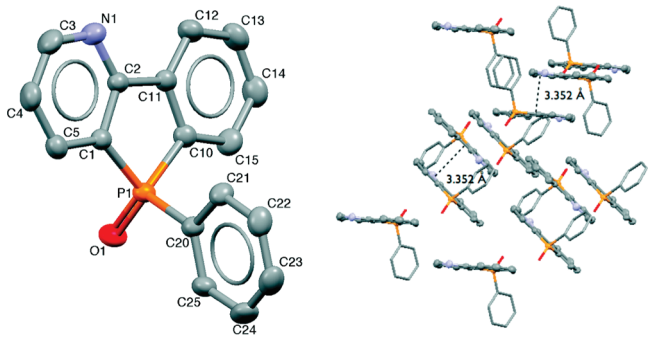

Figure 1. Molecular structure of **1b** (left) and packing diagram (right) in the solid state (50% probability level, H-atoms are omitted for clarity). Selected bond lengths [Å] and angles [deg]: P1−C1 1.804(2), P1−C10 1.809(2), P1−C20 1.799(2), P1−O1 1.4850(16), N1−C2 1.344(3), N1−C3 1.341(3), C1−C2 1.401(3), C3−C4 1.386(4), C4−C5 1.392(4), C1−C5 1.385(3), C2−C11 1.477(3), C10−C11 1.397(3), C11−C12 1.384(3), C12−C13 1.386(4), C13−C14 1.380(4), C14−C15 1.392(4), C10−C15 1.385(3), C20−C21 1.399(3), C21−C22 1.386(3), C22−C23 1.382(4), C23−C24 1.384(4), C24−C25 1.388(3), C20−C25 1.393(3); C1−P1−C10 92.00(10), C1−P1−C20 108.13(9), C10−P1−C20 107.13(10), C1−P1−O1 117.85(10), C10−P1−O1 116.90(10), C20−P1−O1 112.70(10).

those observed in dibenzophosphole oxide **DBPO**. The P−O distance in 4-azadibenzophosphole **4b** (1.4856(17) Å) as well as the bond angles around the phosphorus center are in good agreement with the corresponding bond lengths and angles in **DBPO**.[25] However, in the packing motif, some differences between **1b** and **4b** can be observed. Compound **4b** exhibits somewhat weaker π-stacking interactions (3.44 Å) between inversion-related pairs of enantiomers. Another difference in the packing motif is seen in the overlap between the molecules. In contrast to **1b**, the overlap of the π-systems in **4b** is significant, involving almost the whole annelated ring system. However, no close face-to-face interactions between the phenyl-substituents are observed.

Photophysics and Electrochemistry of Azadibenzophospholes and Oxides. In contrast to the dithienophosphole system, none of the azadibenzophospholes and corresponding oxides shows notable photoluminescence. The azadibenzophospholes **1a**, **3a**, and **4a**, in analogy to dibenzophosphole,[15] were found to oxidize readily in the presence of air (traces) plecluding meaningful UV/vis-spectroscopical studies. The electrochemical properties were determined via cyclic voltammetry, performed under inert gas atmosphere (Table 3). However, significant reduction peaks corresponding to the analogous oxides can be found in all cyclic voltammograms for the azadibenzophospholes (see Supporting Information). Compounds **1a** and **4a** show very similar electrochemical characteristics with irreversible reductions at $E_{red,1/2}$ = −2.69 V and −2.67 V, respectively. In the analyzed

dx.doi.org/10.1021/ic200951x |*Inorg. Chem.* 2011, 50, 6823–6836

range, the 3-aza-isomer **3a** only shows one quasireversible reduction at $E_{red,1/2}$ = −2.55 V. However, multiple irreversible oxidations in the range between $E_{ox,peak}$ = 0.52 and 1.18 V are also observed for all compounds (Table 3).

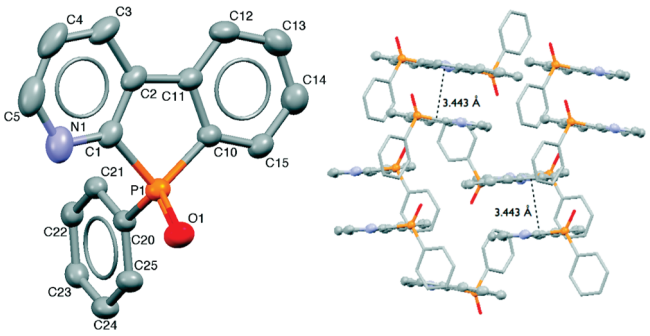

Figure 2. Molecular structure of **4b** (left) and packing diagram (right) in the solid state (50% probability level, H-atoms are omitted for clarity). Selected bond lengths [Å] and angles [deg]: P1−C1 1.809(2), P1−C10 1.804(2), P1−C20 1.800(2), P1−O1 1.4856(17), N1−C1 1.361(3), N1−C5 1.375(4), C1−C2 1.398(3), C2−C3 1.398(3), C3−C4 1.387(4), C4−C5 1.370(5), C2−C11 1.479(3), C10−C11 1.405(3), C11−C12 1.388(3), C12−C13 1.383(4), C13−C14 1.383(4), C14−C15 1.372(4), C10−C15 1.360(3), C20−C21 1.398(3), C21−C22 1.388(3), C22−C23 1.393(3), C23−C24 1.380(3), C24−C25 1.386(3), C20−C25 1.391(3); C1−P1−C10 91.70(11), C1−P1−C20 108.97(10), C10−P1−C20 107.08(10), C1−P1−O1 116.97(10), C10−P1−O1 117.96(10), C20−P1−O1 112.17(10).

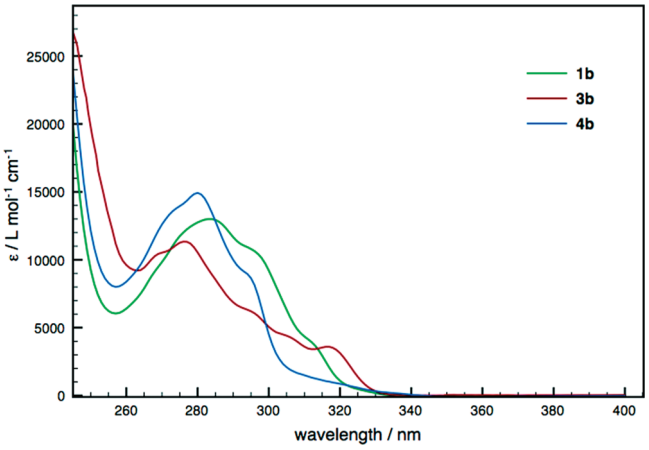

Figure 3. UV/vis absorption spectra of **1b**, **3b**, and **4b** in DCM ($c \sim 10^{-5}$ M).

On the basis of our earlier studies,[14f,20c] we anticipated the phosphole oxide series **1b**, **3b**, and **4b** to be more interesting in terms of their electron-accepting features than the above-mentioned trivalent phospholes **1a**, **3a**, and **4a**. The photophysical properties of the azadibenzophosphole oxides were determined in dilute ($c \sim 10^{-5}$ M) dichloromethane solution, and the UV/vis spectra are depicted in Figure 3. The three phosphole oxides **1b**, **3b**, and **4b** show absorption maxima in a narrow range within the UV-region of the optical spectrum (276−284 nm) with absorption coefficients rising in the order **3b** < **1b** < **4b** (Table 3).

The position of the nitrogen atom in the backbone does influence the charge distribution and concomitantly the transition dipole moment within the molecule, resulting in the observed molar absorptivities. It is interesting to see that **DBPO** shows a significantly smaller absorption coefficient (by a factor of 14−18), probably because of the symmetry, leading to weaker, forbidden electronic transitions.[15] **DBPO** shows a red-shifted absorption maximum ($\Delta\lambda$ = 48−56 nm), but it should be noted that the aza-congeners **1b**, **3b**, and **4b** show weak to medium intensity shoulders in the same range of the optical spectrum. Compared to the dibromo(phenylpyridine)s **9**, **12**, and **15**, the absorption maxima are only red-shifted by ∼10 nm, the onset of absorption, however, experiences a more significant bathochromic shift (∼40 nm), indicating the increased size of the conjugated system by planarization of the backbone.

The electrochemical features of the azadibenzophosphole oxides were determined by cyclic voltammetry (Figure 4).

In contrast to the trivalent phospholes **1a**, **3a**, and **4a**, the corresponding oxides showed no significant oxidation waves in the oxidative regime up to a potential of 1.05 V. Importantly, reversible reduction waves are observed for all phosphole oxides. The azadibenzophosphole oxides show half-step reduction potentials at $E_{red,1/2}$ = −2.30 V (**1b**), −2.14 V (**3b**), and −2.27 V (**4b**), respectively. These values are comparable to those of **IVa**/**b**, indicating a potential application as electron-transporting or hole-blocking material.[11i] The reduction potential of **3b** is lower than those of **1b** and **4b**, indicating that the 4-phenylpyridine backbone stabilizes the LUMO more effectively than the other scaffolds. As anticipated, the reduction potentials decrease significantly upon oxidation (Table 3). Furthermore, it should be noted that there is a clear transition from an irreversible (or quasireversible) to a reversible reduction behavior upon oxidation of the phospholes to the corresponding oxides. Since the materials showed reversible one-electron reduction events,

Table 3. Photophysical and Electrochemical Data for Azadibenzophospholes 1a, 3a, 4a, Corresponding Phosphole Oxides 1b, 3b, 4b and Dibenzophosphole Oxide DBPO[15]

	λ_{abs}[a] [nm]	ε_{max}[a] [L mol^{-1} cm^{-1}]	$E_{red,1/2}$ [V]	$E_{ox,peak}$[e] [V]	E_{LUMO}[f] [eV]	k_{ET}[g] [cm s^{-1}]
1a			−2.69[b]	0.52/0.75/1.08	−2.11	
3a			−2.55[c]	0.68/1.18	−2.25	
4a			−2.67[b]	0.58/1.13	−2.13	
1b	284	13,000	−2.30[d]		−2.50	7.04×10^{-4}
3b	276	11,330	−2.14[d]		−2.66	1.61×10^{-3}
4b	280	14,900	−2.27[d]		−2.53	6.45×10^{-4}
DBPO	332	800	−2.33[d]		−2.47	

[a] UV/vis absorption maxima in CH_2Cl_2. [b] Irreversible reduction half step potentials vs Fc/Fc^+. [c] Quasireversible reduction half-step potential vs Fc/Fc^+. [d] Reversible reduction half-step potential vs Fc/Fc^+. [e] Irreversible oxidation peak potentials vs Fc/Fc^+. [f] Calculated using the ferrocene HOMO level at $-(4.8 + E_{red,1/2})$ eV. [g] Calculated according to Nicholson.[26]

dx.doi.org/10.1021/ic200951x |*Inorg. Chem.* 2011, 50, 6823–6836

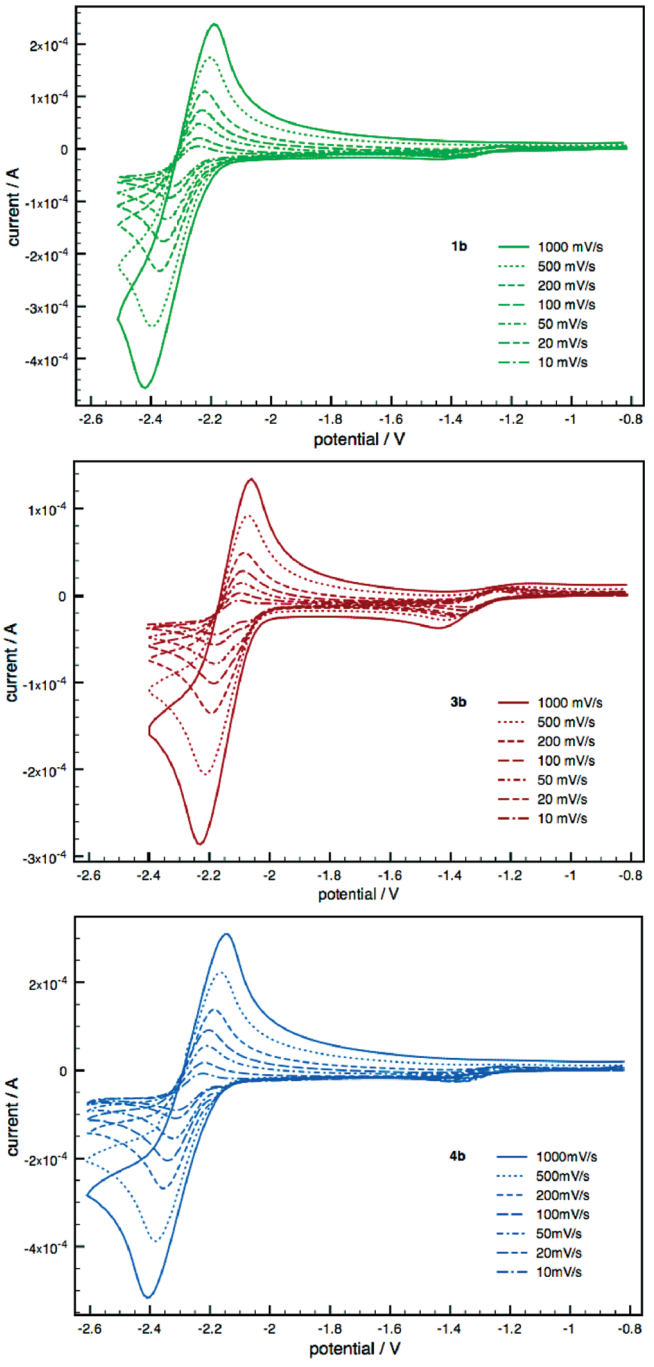

Figure 4. Cyclic voltammograms of **1b** (top), **3b** (center), and **4b** (bottom) in acetonitrile solution, $[NBu_4][PF_6]$ as supporting electrolyte, potential E referenced vs Fc/Fc^+.

assessed by the separation between anodic and cathodic peak potentials, their electron transfer kinetics k_{ET} were evaluated (Table 3).[26] Cyclic voltammograms were measured at different scan rates and k_{ET} extracted from the peak positions and heights. 1-Aza-isomer **1b** and 4-aza-isomer **4b** show similar k_{ET} values ($k_{ET} = 7.04 \times 10^{-4}$ cm s^{-1} (**1b**); 6.45×10^{-4} cm s^{-1} (**4b**)), whereas 3-azadibenzophosphole oxide **3b** exhibits a slightly increased value ($k_{ET} = 1.61 \times 10^{-3}$ cm s^{-1}), probably because of the more polar backbone structure, resulting in higher mobility in an electric field. Overall, the obtained k_{ET} values indicate fast

Table 4. Calculated Energies for Selected Orbitals of the Azadibenzophosphole (1a−4a) and Azadibenzophosphole Oxide (1b−4b) Series[a]

	1a	2a	3a	4a	1b	2b	3b	4b
E_{LUMO}/eV	−1.53	−1.60	−1.75	−1.56	−1.97	−2.16	−2.20	−2.00
E_{HOMO}/eV	−6.38	−6.44	−6.51	−6.37	−6.72	−6.80	−6.99	−6.71
E_{HOMO-1}/eV	−6.45	−6.61	−6.68	−6.41	−7.20	−7.28	−7.26	−7.02
E_{HOMO-2}/eV	−7.11	−7.11	−7.04	−7.01	−7.28	−7.36	−7.35	−7.23

[a] Calculated with Gaussian 03, Revision E.01; B3LYP/6-31G+(d) level of theory.[18]

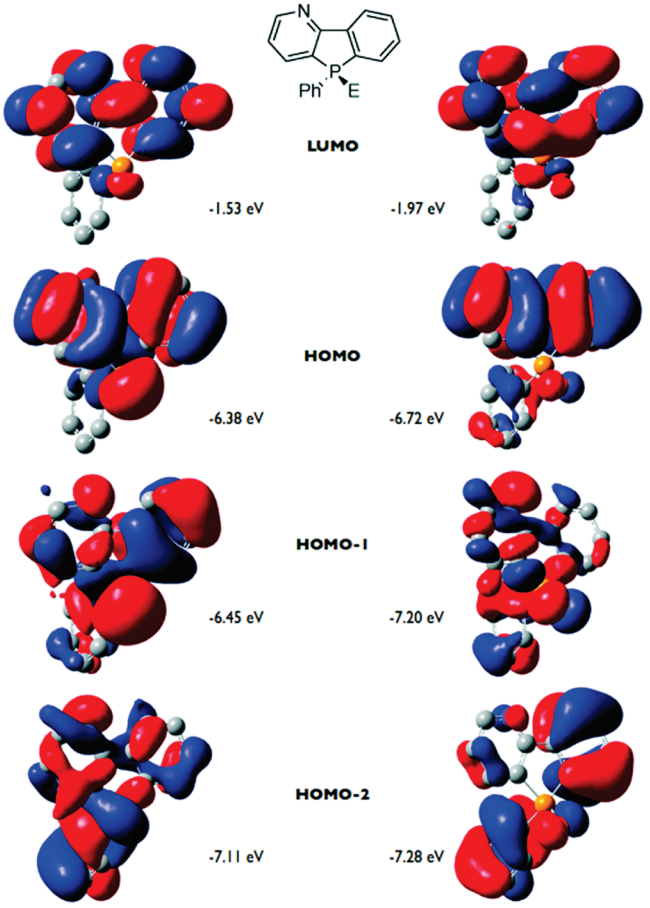

Figure 5. Frontier orbital diagrams for 1-aza-isomers **1a** (left, E = lone pair) and **1b** (right, E = O).

electron transfer processes, well within the range of thiadiazole, thiadiazole-oxide, and -dioxide fused phenanthrenes and pyrenes, which have previously been reported by our group.[7] Rapid electronic processes are beneficial for an application in electronic devices, since charge-transfer phenomena in organic electronics are generally in the nano- to picosecond regime.[27]

Theoretical Calculations. To better understand the electronic and photophysical characteristics, density functional theory (DFT) calculations (B3LYP/6-31G+(d)) have been performed on the azadibenzophospholes **1a**−**4a** and the corresponding oxides **1b**−**4b**, to determine their frontier orbital energies (Table 4).[18] Since the orbital structures are similar within the respective series, only selected orbitals (HOMO-2−LUMO) for 1-azadibenzophosphole **1a** and 1-azadibenzophosphole oxide **1b**

dx.doi.org/10.1021/ic200951x |*Inorg. Chem.* 2011, 50, 6823–6836

Table 5. Calculated Electronic Transitions and Oscillator Strengths *f* for Azadibenzophosphole Oxides 1b, 3b, and 4b[a]

	1b	3b	4b
λ [nm]	303	305	304
f	0.030	0.010	0.004
transition	HOMO−LUMO	HOMO-1−LUMO	HOMO−LUMO
λ [nm]	285	296	292
f	0.088	0.036	0.028
transition	HOMO-2−LUMO	HOMO−LUMO	HOMO-1−LUMO+1
λ [nm]	277	284	286
f	0.006	0.008	0.062
transition	HOMO−LUMO+1	HOMO-2−LUMO	HOMO−LUMO+1

[a] TD-DFT calculations with Gaussian 03, Revision E.01; B3LYP/6-31G+(d) level of theory.[18]

are depicted in Figure 5 (for additional orbital diagrams, see Supporting Information). The LUMO and HOMO orbital diagrams show a major contribution from the π-system of the backbone for both 1-aza-isomer **1a** and oxide **1b**.

For **1a**, the highest occupied molecular orbital (HOMO) also shows significant contribution from the phosphorus lone pair. The HOMO-1 orbitals show contribution from the nitrogen lone pair for both the phospholes and phosphole oxides. In the case of **1a**, the HOMO-1 also shows some contribution from the nitrogen lone pair, whereas in **1b**, the π-system and the phenyl substituents are major contributors. In contrast to **1b**, the HOMO-2 level in **1a** still shows some nitrogen lone pair character. In accordance with the electrochemical data, the calculations clearly indicate that the oxidation of the phospholes lead to significant stabilization of the LUMO energy levels ($\Delta E \sim 0.4-0.5$ eV). It is also interesting to note that the calculated energies are very similar for the respective pairs **1a**/**4a**, **2a**/**3a**, **1b**/**4b**, and **2b**/**3b**. The electrochemical data confirm the similarity for the sets **1a**/**4a** and **1b**/**4b** (Table 4), giving rise to the assumption that 2-aza-isomer **2a**,**b** (not obtained synthetically) likely exhibits electrochemical properties comparable to the 3-aza-congener **3a**,**b**. In addition to the orbital energy levels, the electronic spectra for the synthetically accessible azadibenzophosphole oxides **1b**, **3b**, and **4b** were modeled via TD-DFT calculations (Table 5). The agreement between the calculated and measured UV/vis spectra is fair; all calculated spectra show onsets within 10−20 nm of the experimentally determined data, resulting from HOMO−LUMO (**1b**, **4b**) or HOMO-1−LUMO (**3b**) transitions. Other significant transitions are listed in Table 5 and include transitions from the HOMO-2−HOMO orbitals to the LUMO or LUMO+1 energy levels, respectively. Although the experimentally observed absorptivities are not matched very well by the calculated data, it should be noted that the calculated absorption coefficients agree better with experimental data in the low-energy portion (275−350 nm) of the absorption spectra. In the high-energy range of the spectra (240−270 nm); however, the correlation between calculated and measured photophysical data is poor.

3. Chemical Modification of the Azadibenzophosphole Scaffold. *Attempted Reduction of 1-Azadibenzophosphole Oxide* ***1b***. As shown in previous work, phosphole oxides can often be reduced to the corresponding trivalent species, which presents an interesting way to functionalize the phosphorus

Scheme 4. Reactivity of Azadibenzophospholes 1b, 3b, and 4b toward Pt(II)

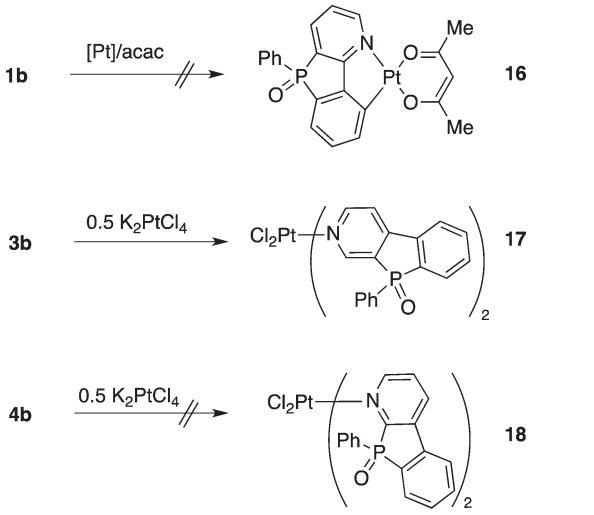

center after, for example, a preceding cross-coupling reaction, generally requiring protection of the phosphorus to avoid poisoning of the catalyst.[19c] The reduction of dithienophospholes is accomplished via treatment with borane and subsequent addition of triethylamine. In the case of the azadibenzophospholes, this approach was anticipated to be not suitable, because of the presence of the imine-nitrogen in the backbone, which would readily coordinate to the borane. The approach investigated for the reduction of the phosphole oxide moiety in this study, involved the treatment of 1-aza-isomer **1b** with tri*n*-butylphosphane.[28] Compound **1b** was dissolved in freshly degassed benzene-D_6 and an excess of phosphane added and sonicated for 1 h at 60 °C. However, ^{31}P NMR spectroscopy did not provide the resonance corresponding to the reduced, trivalent phosphole, suggesting that reduction cannot be achieved according to the outlined procedure, potentially because of the electron-poor nature of the backbone, which could strengthen the P−O bond.[20b,c]

Metal Coordination. The presence of a Lewis-basic nitrogen center in the backbone of azadibenzophospholes gives rise to a potential application for the materials as *N*-donor ligands in combination with transition metals. To explore the coordination behavior of the azadibenzophosphole scaffold and the resulting effect of the functionalization on the photophysical and electronic properties, different Pt-species were reacted with the azadibenzophosphole oxides. Since the 1-azadibenzophosphole oxide **1b** incorporates a backbone analogous to 2-phenylpyridine, cyclometalation was attempted (Scheme 4). It has been shown that cyclometalation of phenylpyridines with platinum gives rise to phosphorescence, tunable in color via the electronic features of the chelate ligand.[29]

However, treatment of the 1-aza-isomer **1b** with either [Pt(acac)(DMSO)Cl], or K_2PtCl_4/acac (acac = acetylacetonate), according to reported procedures,[29a,b] did not result in the formation of the target complex **16**. Only starting materials or inseparable decomposition products could be observed under varying conditions, respectively.

It should be noted that the reported procedures use non-bridged phenylpyridines as starting materials, giving rise to the assumption that the phenylpyridine-unit in **1b** is an unsuitable scaffold for cyclometalation. The lack of success in the synthesis

of **16** can be rationalized by the distortion of the phenylpyridine backbone because of the bridging phosphorus, widening the bite-angle of the prospective ligand, thus providing an unfavorable geometry for cyclometalation with platinum. Since the 3- and 4-aza-isomers **3b** and **4b** possess potentially accessible nitrogen donor centers, the Pt-pyridine complexes **17** and **18** (Scheme 4) were established as our next synthetic targets. The azadibenzophosphole oxides **3b** and **4b** were dissolved in ethanol and treated with K_2PtCl_4, dissolved in water at 50 °C. In the case of the 3-aza-isomer **3b**, a precipitate started to form after 15 min, whereas no visible change was observed in the reaction with **4b**, even after stirring for 16 h at 50 °C. After workup, NMR spectroscopy on crude product **18** revealed the presence of starting material **4b** only. The inaptness of **4b** to act as a ligand can be rationalized with its steric and electronic characteristics; quite possibly, the environment around the nitrogen is sterically too congested to accommodate a metal in its vicinity. In terms of electronic properties, the nitrogen lone pair likely exhibits reduced donor-capability because of the electron-withdrawing effect of the oxidized phosphorus in *ortho*-position.

However, more success was observed in the synthesis of Pt-complex **17**, which was obtained in moderate yield (62%) as white powder. The ^{31}P NMR resonance of **17** (δ ^{31}P = 32.1 ppm) is shifted upfield by 1.9 ppm compared to that of starting material **3b** (δ ^{31}P = 34.0 ppm). Furthermore, the ^{1}H NMR shifts of the hydrogen atoms adjacent to the nitrogen, showing a downfield displacement by ~0.2 ppm, as well as the occurrence of a ^{195}Pt NMR resonance (δ ^{195}Pt = −312.2 ppm), indicated the successful formation of complex **17**. The ^{195}Pt NMR resonance is shifted significantly downfield compared to *cis*-$[Pt(py)_2Cl_2]$ (δ ^{195}Pt = −2014 ppm), probably because of the electron-withdrawing nature of the phosphole oxide-containing ligand.[30] *trans*-$[Pt(py)_2Cl_2]$ shows a ^{195}Pt NMR resonance a δ ^{195}Pt = −1964 ppm,[30] allowing no clear assignment of the configuration of complex **17**. However, *cis*-configured Pt-complexes are commonly formed under the applied reaction conditions.[31] The electrochemical properties of **17** were probed via cyclic voltammetry (see Supporting Information). The analysis revealed multiple irreversible reduction events ($E_{red,peak}$ = −1.80 V, −2.06 V, −2.22 V, −2.58 V) probably because of sequential reduction of the ligands and the metal center. Furthermore, an irreversible oxidation ($E_{ox,peak}$ = −0.96 V) was observed, likely caused by oxidation of the metal center.[32] The photophysical properties of compound **17** were investigated by means of UV/vis spectroscopy (see Supporting Information). Very strong absorption bands in the UV range of the optical spectrum were observed (λ_{abs} = 333 nm, ε_{333} = 148,700 L mol^{-1} cm^{-1}; λ_{abs} = 287 nm, ε_{287} = 115,700 L mol^{-1} cm^{-1}; λ_{abs} = 255 nm, ε_{255} = 290,400 L mol^{-1} cm^{-1}), probably because of electronic decoupling of the ligands into two independent chromophores. Similar behavior with a significant increase of the molar absorptivity has been observed for a dithienophosphole oxide-capped, biphenyl bridged oligomer;[33] however, the increase in the extinction coefficient is much more substantial for **17**, possibly because of metal to ligand charge transfer (MLCT) nature of the bands.[34] The absorption wavelengths are in fair agreement with those observed in *cis*-$[Pt(py)_2Cl_2]$ (λ_{abs} = 310 nm, ε_{310} = 1800 L mol^{-1} cm^{-1}; λ_{abs} = 280 nm, ε_{280} = 6660 L mol^{-1} cm^{-1}; λ_{abs} = 238 nm, ε_{238} = 12,100 L mol^{-1} cm^{-1})[34] and azadibenzophosphole oxide **3b** (Figure 3), albeit with significantly higher extinction coefficients for **17**. The pronounced changes in the absorption behavior upon metal complexation suggest a potential use for **3b** in the context of molecular sensors.[35]

Scheme 5. Reactivity of 4a toward MeOTf and Au(tht)Cl

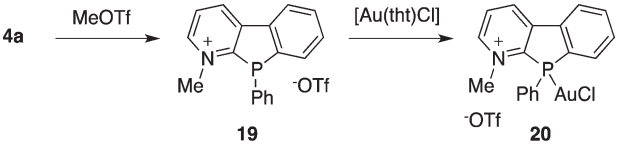

Reactivity Toward a Lewis-Acid and Subsequent Metal Coordination. Since the trivalent azadibenzophospholes incorporate two Lewis-basic functionalities, that is, the nitrogen and the phosphorus center, their relative basicity was investigated by treatment of 4-azadibenzophosphole **4a** with 1 equiv of methyltriflate (MeOTf), added in five increments. After each addition, a sample was taken and a ^{31}P NMR spectrum measured showing a clean conversion of **4a** (δ ^{31}P = −14.8 ppm) to a single product (δ ^{31}P = −10.4 ppm) upon addition of 1 equiv of MeOTf (see Supporting Information). Previous studies on the dithienophosphole[36] and related systems[14f,20c] have shown that the methylation of the phosphorus center leads to a downfield shift of the ^{31}P NMR resonance by ~34−43 ppm and the occurrence of a ^{1}H NMR signal (doublet) with a characteristic coupling constant of ~15 Hz. In the case presented here, the difference in the ^{31}P NMR resonance is merely 4.5 ppm, and the ^{1}H NMR signal corresponding to the methyl-group shows no coupling (singlet). These results clearly support the methylation at the nitrogen, rather than the phosphorus center (Scheme 5), indicating that the imine-fragment in the backbone is significantly more Lewis-basic than the phosphorus center.

This result is consistent with experimentally determined pK_a values for the conjugate acids of 1-methylphosphole (pK_a = 0.5)[37] and pyridine (pK_a = 5.2),[38] indicating that pyridine is a stronger base than phosphole. To investigate whether the phosphorus center is still basic enough for further functionalization, the MeOTf-adduct **19** was subsequently treated with 1 equiv of [Au(tht)Cl] (tht = tetrahydrothiophene; Scheme 5) to give gold-complex **20** as off-white, crystalline solid in moderate isolated yield (54%). The formation of **20** was indicated by a significant shift of the ^{31}P NMR resonance (δ ^{31}P = 25.8 ppm), clearly showing that a reaction occurred at the phosphorus center. The electrochemical properties of **20** were investigated via cyclic voltammetry (see Supporting Information). The analysis revealed two irreversible reduction events ($E_{red,peak}$ = −1.21 V, −2.28 V, vs Fc/Fc$^+$) likely because of sequential reduction of the metal center and the ligand. Furthermore, an irreversible oxidation ($E_{ox,peak}$ = 0.13 V, vs Fc/Fc$^+$) occurred after the first reductive sweep, indicating decomposition of the complex under reductive conditions. The appearance of the oxidative wave is the result of the oxidation of the decomposition products formed during the reductive sweeps. The photophysical properties of compound **20** were investigated by means of UV/vis spectroscopy (see Supporting Information). Medium to strong absorption bands in the UV range of the optical spectrum were observed (λ_{max} = 337 nm, ε_{337} = 4180 L mol^{-1} cm^{-1}; $\lambda_{shoulder}$ = 299 nm, ε_{299} = 19,720 L mol^{-1} cm^{-1}; λ_{max} = 290 nm, ε_{299} = 21,440 L mol^{-1} cm^{-1}), that relate well to the absorption features seen in the Pt-complex **17** and azadibenzophosphole oxide **4b**. The increase in molar absorptivity compared to **4b** is likely also a result of the MLCT nature of the bands.[34]

Halogenation and Cross-Coupling. We were interested to see whether it was possible to further functionalize the backbone of the azadibenzophosphole scaffold by halogenation, which would subsequently allow extension of the building blocks via cross-

dx.doi.org/10.1021/ic200951x |*Inorg. Chem.* 2011, 50, 6823–6836

Scheme 6. Bromination and Subsequent Cross-Coupling of 4b

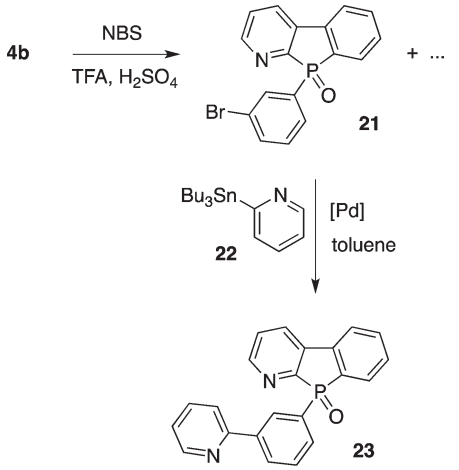

coupling reactions with aromatic groups. Previous studies have shown that extension of the conjugated scaffold leads to dramatically altered photophysical and electronic properties, which allows tuning of these features to a targeted application.[19c,f,33] It should be noted that substituted dibenzophosphole oxides are usually synthesized via precursor routes, starting from suitably functionalized biphenyls that are subsequently transformed into the phosphole derivatives.[39] However, because of the difference of the backbone, we anticipated that direct halogenation with *N*-bromosuccinimide (NBS) may be possible for the azadibenzophospholes. Initially, standard conditions, established for the bromination of dithienophosphole **6**, were applied.[19c] However, no conversion was observed after treatment of **4b** with NBS in refluxing chloroform/acetic acid or DMF (rt or 100 °C). This result can be rationalized by the electron-poor nature of the azadibenzophosphole oxide system, rendering it strongly deactivated for electrophilic attack by the brominating agent. According to a procedure for the bromination of deactivated arenes,[40] the bromination of **4b** was then attempted with 1.6 equiv of NBS in trifluoroacetic acid (TFA)/sulfuric acid in the dark overnight. After workup, NMR spectroscopy indicated the formation of several species, one of which could be isolated in 32% yield, and identified as monobrominated **21** by ^{1}H NMR spectroscopy (Scheme 6). To establish where the functionalization specifically took place, the ^{13}C NMR spectrum was analyzed. The number of signals clearly proved that a desymmetrization of the exocyclic phenyl-substituent occurred, meaning that the bromination must have unexpectedly occurred at the *ortho*- or *meta*-position of the phenyl ring. The formation of the brominated species was accompanied by an upfield shift of the ^{31}P NMR resonance (δ ^{31}P = 23.6 (**21**); cf. **4b**: δ ^{31}P = 25.1 ppm), but the site of the bromination (*meta*) was finally unambiguously proven by single-crystal X-ray crystallography (Figure 6; Table 1). The molecular structure of **21** in the solid state corresponds well to the ones described above, exhibiting a planar backbone with little bond length alternation.

All bond lengths and angles are in good agreement with the structures for 1- and 4-aza-isomers **1b** and **4b**, as well as dibenzo-analogue **DBPO**. The packing motif of **21** shows close π-stacking interactions (3.37 Å) between the π-systems of pairs of enantiomers, as seen previously. Furthermore, the structure exhibits face-to-face interactions (3.60 Å) between the phenyl-groups.

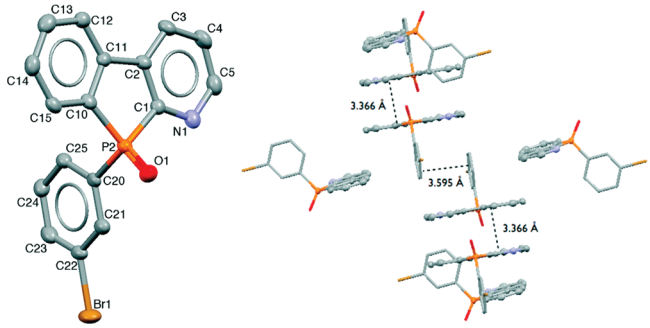

Figure 6. Molecular structure of **21** (left) and packing diagram (right) in the solid state (50% probability level, H-atoms are omitted for clarity). Selected bond lengths [Å] and angles [deg]: P2−C1 1.813(5), P2−C10 1.805(5), P2−C20 1.800(5), P2−O1 1.478(4), N1−C1 1.340(6), N1−C5 1.362(7), C22−Br1 1.904(5), C1−C2 1.393(6), C2−C3 1.393(7), C3−C4 1.379(7), C4−C5 1.385(7), C2−C11 1.478(6), C10−C11 1.404(6), C11−C12 1.395(6), C12−C13 1.381(7), C13−C14 1.385(8), C14−C15 1.386(7), C10−C15 1.381(7), C20−C21 1.397(6), C21−C22 1.378(7), C22−C23 1.375(8), C23−C24 1.393(7), C24−C25 1.387(6), C20−C25 1.404(7); C1−P2−C10 91.4(2), C1−P2−C20 106.2(2), C10−P2−C20 109.0(2), C1−P2−O1 117.9(2), C10−P2−O1 117.0(2), C20−P1−O1 113.1(2).

Subsequently, compound **21** was subjected to a proof-of-principle Stille cross-coupling with commercially available 2-tri-*n*-butylstannylpyridine **22** to investigate whether the brominated 4-aza-derivative could be further functionalized (Scheme 6). The reaction proceeded cleanly, and the azadibenzophosphole-functionalized phenylpyridine derivative **23** was obtained as white solid in good isolated yield (76%). The successful formation of **23** was indicated by occurrence of the expected additional ^{1}H and ^{13}C NMR resonances as well as a downfield shift of the ^{31}P NMR resonance (δ ^{31}P = 25.2 ppm), compared to starting material **21** (δ ^{31}P = 23.6 ppm).

CONCLUSION

In conclusion, we have succeeded in synthesizing and characterizing a series of novel azadibenzophospholes and -phosphole oxides and their respective precursors. The azadibenzophosphole oxides in particular, exhibit intriguing electrochemical properties, such as reversible reduction potentials with fast electron-transfer rates, comparable to established electron-transporting or hole-blocking materials, making the new compounds promising materials for an application in organic electronics. These results were supported by DFT calculations. It has been shown that the position of the nitrogen in the backbone has some influence on the electrochemical and photophysical features, but significant impact of the coordination behavior toward transition metals. Pt(II)-coordination to an extended 3-azadibenzophosphole oxide led to significantly increased absorption features, when compared with established pyridine complexes of Pt^{2+}, whereas the other isomers do not show any utility as ligands, largely because of the results of the steric bulk or distortion of the scaffold, respectively. The relative basicity of the nitrogen to the trivalent phosphorus center in the scaffold has been determined qualitatively and is in agreement to the expected trend for pyridine and phosphole species. Finally, an interesting regiochemistry for bromination reactions has been observed, giving rise to a potential incorporation of the electroactive azadibenzophosphole scaffold as a pendant side chain into conjugated oligomers.

dx.doi.org/10.1021/ic200951x |*Inorg. Chem.* 2011, 50, 6823–6836

The feasibility of cross-coupling reactions of a brominated species has been demonstrated and further investigation with regard to the ligand properties of **23** as well as the incorporation of the azadibenzophosphole-functionalized phenylpyridine **21** into π-conjugated oligomers are currently underway and will be reported in due course. The same is true for the verification of the electron-transfer capability of the azadibenzophospholes **1b**, **3b**, and **4b** in corresponding devices.

■ ASSOCIATED CONTENT

Supporting Information. X-ray crystallographic data of the dibromo(phenylpyridine)s **12** and **15**; photophysics and electrochemistry of the dibromo(phenylpyridine)s **9**, **12**, and **15**; cyclic voltammograms of azadibenzophospholes **1a**, **3a**, and **4a**; ^{31}P NMR spectra of **4a** before and after addition of MeOTf; frontier orbital diagrams for compound **2a**/**b**, **3a**/**b** and **4a**/**b**; cyclic voltammograms and UV−vis absorption spectra of **17** and **20**. This material is available free of charge via the Internet at http://pubs.acs.org.

■ AUTHOR INFORMATION

Corresponding Author
*E-mail: thomas.baumgartner@ucalgary.ca.

■ ACKNOWLEDGMENT

Financial support by NSERC of Canada and the Canada Foundation for Innovation (CFI) is gratefully acknowledged. We also thank Alberta Ingenuity, now part of Alberta Innovates-Technology Futures, for a graduate scholarship (S.D.) and a New Faculty Award (T.B.). Thanks to Prof. T. Sutherland for his help with the electrochemical studies, and Dr. T. Linder for helpful discussions with regard to X-ray crystallography.

■ REFERENCES

(1) (a) Anthony, J. E. *Chem. Rev.* **2006**, *106*, 5028–5048. (b) Anthony, J. E. *Angew. Chem., Int. Ed.* **2008**, *47*, 452–483. (c) Subramanian, S.; Park, S. K.; Parkin, S. R.; Podzorov, V.; Jackson, T. N.; Anthony, J. E. *J. Am. Chem. Soc.* **2008**, *130*, 2706–2707. (d) Kim, D. H.; Lee, D. Y.; Lee, H. S.; Lee, W. H.; Kim, Y. H.; Han, J. I.; Cho, K. *Adv. Mater.* **2007**, *19*, 678–682. (e) Tang, M. L.; Reichardt, A. D.; Miyaki, N.; Stoltenberg, R. M.; Bao, Z. *J. Am. Chem. Soc.* **2008**, *130*, 6064–6065.

(2) (a) Perepichka, I. F.; Perepichka, D. F.; Meng, H.; Wudl, F. *Adv. Mater.* **2005**, *17*, 2281–2305.(b) Müllen, K.; Scherf, U. *Organic Light Emitting Devices*; Wiley-VCH: Weinheim, 2006. (c) Veinot, J. G. C.; Marks, T. J. *Acc. Chem. Res.* **2005**, *38*, 632–643.(d) Klauk, H. *Organic Electronics*; Wiley-VCH: Weinheim, 2006.

(3) (a) Gao, P.; Beckmann, D.; Tsao, H. N.; Feng, X.; Enkelmann, V.; Baumgarten, M.; Pisula, W.; Müllen, K. *Adv. Mater.* **2009**, *21*, 213–216. (b) Gao, P.; Feng, X.; Yang, X.; Enkelmann, V.; Baumgarten, M.; Müllen, K. *J. Org. Chem.* **2008**, *73*, 9207–9213. (c) Takimiya, K.; Ebata, H.; Sakamoto, K.; Izawa, T.; Otsubo, T.; Kunugi, Y. *J. Am. Chem. Soc.* **2006**, *128*, 12604–12605. (d) Ebata, H.; Izawa, T.; Miyazaki, E.; Takimiya, K.; Ikeda, M.; Kuwabara, H.; Yui, T. *J. Am. Chem. Soc.* **2007**, *129*, 15732–15733. (e) Zhang, X.; Cotê, A. P.; Matzger, A. J. *J. Am. Chem. Soc.* **2005**, *127*, 10502–10503.

(4) (a) Jacob, J.; Sax, S.; Piok, T.; List, E. J. W.; Grimsdale, A. C.; Müllen, K. *J. Am. Chem. Soc.* **2004**, *126*, 6987–6995. (b) Zhou, Y.; Liu, W.-J.; Ma, Y.; Wang, H.; Qi, L.; Cao, Y.; Wang, J.; Pei, J. *J. Am. Chem. Soc.* **2007**, *129*, 12386–12387.

(5) (a) Skotheim, T. A.; Reynolds, J. R. *Handbook of Conducting Polymers*, 3rd ed.; CRC Press: Boca Raton, FL, 2006. (b) Blouin, N.; Leclerc, M. *Acc. Chem. Res.* **2008**, *41*, 1110–1119. (c) Boudreault, P.-L. T.; Beaupré, S.; Leclerc, M. *Polym. Chem.* **2010**, *1*, 127–136.

(6) (a) Usta, H.; Facchetti, A.; Marks, T. J. *Org. Lett.* **2008**, *10*, 1385–1388. (b) Ren, Y.; Dienes, Y.; Hettel, S.; Parvez, M.; Hoge, B.; Baumgartner, T. *Organometallics* **2009**, *28*, 734–740. (c) Ahmed, E.; Earmme, T.; Ren, G.; Jenekhe, S. A. *Chem. Mater.* **2010**, *22*, 5786–5796.

(7) (a) Linder, T.; Sutherland, T. C.; Baumgartner, T. *Chem.—Eur. J.* **2010**, *16*, 7101–7105. (b) Linder, T.; Badiola, E.; Baumgartner, T.; Sutherland, T. C. *Org. Lett.* **2010**, *12*, 4520–4523.

(8) (a) Newman, C. R.; Frisbie, C. D.; da Silva Filho, D. A.; Brédas, J.-L.; Ewbank, P. C.; Mann, K. R. *Chem. Mater.* **2004**, *16*, 4436–4451. (b) Kappaun, S.; Slugovc, C.; List, E. J. W. *Int. J. Mol. Sci.* **2008**, *9*, 1527–1547.

(9) (a) Bao, Z.; Lovinger, A. J.; Brown, J. *J. Am. Chem. Soc.* **1998**, *120*, 207–208. (b) Sakamoto, Y.; Suzuki, T.; Kobayashi, M.; Gao, Y.; Fukai, Y.; Inoue, Y.; Sato, F.; Tokito, S. *J. Am. Chem. Soc.* **2004**, *126*, 8138–8140. (c) Swartz, C. R.; Parkin, S. R.; Bullock, J. E.; Anthony, J. E.; Mayer, A. C.; Malliaras, G. G. *Org. Lett.* **2005**, *7*, 3163–3166.

(10) (a) Usta, H.; Risko, C.; Wang, Z.; Huang, H.; Deliomeroglu, M. K.; Zhukhovitskiy, A.; Facchetti, A.; Marks, T. J. *J. Am. Chem. Soc.* **2009**, *131*, 5586–5608. (b) Jones, B. A.; Facchetti, A.; Wasielewski, M. R.; Marks, T. J. *Chem. Mater.* **2007**, *19*, 2703–2705. (c) Andrew, T. L.; Cox, J. R.; Swager, T. M. *Org. Lett.* **2011**, *12*, 5302–5305.

(11) (a) Hsu, F.-M.; Chien, C.-H.; Shih, P.-I.; Shu, C.-F. *Chem. Mater.* **2009**, *21*, 1017–1022. (b) Jeon, S. O.; Yook, K. S.; Joo, C. W.; Lee, J. Y. *Adv. Funct. Mater.* **2009**, *19*, 3644–3649. (c) Hsu, F.-M.; Chien, C.-H.; Shu, C.-F.; Lai, C.-H.; Hsieh, C.-C.; Wang, K.-W.; Chou, P.-T. *Adv. Funct. Mater.* **2009**, *19*, 2834–2843. (d) Chien, C.-H.; Chen, C.-K.; Hsu, F.-M.; Shu, C.-F.; Chou, P.-T.; Lai, C.-H. *Adv. Funct. Mater.* **2009**, *19*, 560–566. (e) Tsuji, H.; Sato, K.; Sato, Y.; Nakamura, E. *J. Mater. Chem.* **2009**, *19*, 3364–3366. (f) Chou, H.-H.; Cheng, C.-H. *Adv. Mater.* **2010**, *22*, 2468–2471. (g) Jeon, S. O.; Yook, K. S.; Joo, C. W.; Lee, J. Y. *Adv. Mater.* **2010**, *22*, 1872–1876. (h) Koech, P. K.; Polikarpov, E.; Rainbolt, J. E.; Cosimbescu, L.; Swensen, J. S.; Von Ruden, A. L.; Padmaperuma, A. B. *Org. Lett.* **2010**, *12*, 5534–5537. (i) Von Ruden, A. L.; Cosimbescu, L.; Polikarpov, E.; Koech, P. K.; Swensen, J. S.; Wang, L.; Darsell, J. T.; Padmaperuma, A. B. *Chem. Mater.* **2010**, *22*, 5678–5686.

(12) (a) Wood, T. K.; Piers, W. E.; Keay, B. A.; Parvez, M. *Angew. Chem., Int. Ed.* **2009**, *48*, 4009–4012. (b) Wood, T. K.; Piers, W. E.; Keay, B. A.; Parvez, M. *Chem.—Eur. J.* **2010**, *16*, 12199–12206. (c) Chen, J.; Kampf, J. W.; Ashe, A. J., III *Organometallics* **2008**, *27*, 3639–3641.

(13) (a) Miao, S.; Appleton, A. L.; Berger, N.; Barlow, S.; Marder, S. R.; Hardcastle, K. I.; Bunz, U. H. F. *Chem.—Eur. J.* **2009**, *15*, 4990–4993. (b) Bunz, U. H. F. *Chem.—Eur. J.* **2009**, *15*, 6780–6789. (c) Lian, Z.; Tang, Q.; Xu, J.; Miao, Q. *Adv. Mater.* **2011**, *23*, 1535–1539. (d) Richards, G. J.; Hill, J. P.; Subbaiyan, N. K.; D'Souza, F.; Karr, P. A.; Elsegood, M. R. J.; Teat, S. J.; Mori, T.; Ariga, K. *J. Org. Chem.* **2009**, *74*, 8914–8923.

(14) (a) Fukazawa, A.; Hara, M.; Son, T.; Okamoto, E.-C.; Xu, C.; Tamao, K.; Yamaguchi, S. *Org. Lett.* **2008**, *10*, 913–916. (b) Fukazawa, A.; Ichihashi, Y.; Kosaka, Y.; Yamaguchi, S. *Chem.—Asian J.* **2009**, *4*, 1729–1740. (c) Saito, A.; Miyajima, T.; Nakashima, M.; Fukushima, T.; Kaji, H.; Matano, Y.; Imahori, H. *Chem.—Eur. J.* **2009**, *15*, 10000–10004. (d) Miyajima, T.; Matano, Y.; Imahori, H. *Eur. J. Org. Chem.* **2008**, 255–259. (e) Matano, Y.; Miyajima, T.; Fukushima, T.; Kaji, H.; Kimura, Y.; Imahori, H. *Chem.—Eur. J.* **2008**, *14*, 8102–8115. (f) Dienes, Y.; Eggenstein, M.; Kárpáti, T.; Sutherland, T. C.; Nyulászi, L.; Baumgartner, T. *Chem.—Eur. J.* **2008**, *14*, 9878–9889.

(15) Su, H.-C.; Fadhel, O.; Yang, C.-J.; Cho, T.-Y.; Fave, C.; Hissler, M.; Wu, C. C.; Réau, R. *J. Am. Chem. Soc.* **2006**, *128*, 983–995.

(16) (a) De Pascali, S. A.; Papadia, P.; Ciccarese, A.; Pacifico, C.; Fanizzi, F. P. *Eur. J. Inorg. Chem.* **2005**, 788–796. (b) Rochon, F. D.; Bensimon, C.; Tessier, C. *Inorg. Chim. Acta* **2008**, *361*, 16–28.

(17) Usón, R.; Laguna, A.; Laguna, M. *Inorg. Synth.* **1989**, *26*, 85–91.

(18) Frisch, M. J.; Trucks, G. W.; Schlegel, H. B.; Scuseria, G. E.; Robb, M. A.; Cheeseman, J. R.; Montgomery, Jr., J. A.; Vreven, T.; Kudin, K. N.; Burant, J. C.; Millam, J. M.; Iyengar, S. S.; Tomasi, J.;

Barone, V.; Mennucci, B.; Cossi, M.; Scalmani, G.; Rega, N.; Petersson, G. A.; Nakatsuji, H.; Hada, M.; Ehara, M.; Toyota, K.; Fukuda, R.; Hasegawa, J.; Ishida, M.; Nakajima, T.; Honda, Y.; Kitao, O.; Nakai, H.; Klene, M.; Li, X.; Knox, J. E.; Hratchian, H. P.; Cross, J. B.; Bakken, V.; Adamo, C.; Jaramillo, J.; Gomperts, R.; Stratmann, R. E.; Yazyev, O.; Austin, A. J.; Cammi, R.; Pomelli, C.; Ochterski, J. W.; Ayala, P. Y.; Morokuma, K.; Voth, G. A.; Salvador, P.; Dannenberg, J. J.; Zakrzewski, V. G.; Dapprich, S.; Daniels, A. D.; Strain, M. C.; Farkas, O.; Malick, D. K.; Rabuck, A. D.; Raghavachari, K.; Foresman, J. B.; Ortiz, J. V.; Cui, Q.; Baboul, A. G.; Clifford, S.; Cioslowski, J.; Stefanov, B. B.; Liu, G.; Liashenko, A.; Piskorz, P.; Komaromi, I.; Martin, R. L.; Fox, D. J.; Keith, T.; Al-Laham, M. A.; Peng, C. Y.; Nanayakkara, A.; Challacombe, M.; Gill, P. M. W.; Johnson, B.; Chen, W.; Wong, M. W.; Gonzalez, C.; Pople, J. A. *Gaussian 03*, Revision E.01; Gaussian Inc.: Wallingford, CT, 2007.

(19) (a) Baumgartner, T.; Neumann, T.; Wirges, B. *Angew. Chem., Int. Ed.* **2004**, *43*, 6197–6201. (b) Baumgartner, T.; Bergmans, W.; Kárpáti, T.; Neumann, T.; Nieger, M.; Nyulászi, L. *Chem.—Eur. J.* **2005**, *11*, 4687–4699. (c) Dienes, Y.; Durben, S.; Kárpáti, T.; Neumann, T.; Englert, U.; Nyulászi, L.; Baumgartner, T. *Chem.—Eur. J.* **2007**, *13*, 7487–7500. (d) Romero-Nieto, C.; Merino, S.; Rodríguez-López, J.; Baumgartner, T. *Chem.—Eur. J.* **2009**, *15*, 4135–4145. (e) Dienes, Y.; Englert, U.; Baumgartner, T. *Z. Anorg. Allg. Chem.* **2009**, *635*, 238–244. (f) Romero-Nieto, C.; Durben, S.; Kormos, I. M.; Baumgartner, T. *Adv. Funct. Mater.* **2009**, *19*, 3625–3631.

(20) (a) Ren, Y.; Linder, T.; Baumgartner, T. *Can. J. Chem.* **2009**, *87*, 1222–1229. (b) Ren, Y.; Baumgartner, T. *Chem.—Asian J.* **2010**, *5*, 1918–1929. (c) Ren, Y.; Baumgartner, T. *J. Am. Chem. Soc.* **2011**, *133*, 1328–1340.

(21) Baxter, P. N. W. *Chem.—Eur. J.* **2003**, *9*, 2531–2541.

(22) (a) Rao, Y. L.; Amarne, H.; Zhao, S. B.; McCormick, T. M.; Martic, S.; Sun, Y.; Wang, R. Y.; Wang, S. *J. Am. Chem. Soc.* **2008**, *130*, 12898–12900. (b) Baik, C.; Hudson, Z. M.; Amarne, H.; Wang, S. *J. Am. Chem. Soc.* **2009**, *131*, 14549–14559.

(23) Affandi, S.; Nelson, J. H.; Alcock, N. W.; Howard, O. W.; Alyea, E. C.; Sheldrick, G. M. *Organometallics* **1988**, *7*, 1724–1734.

(24) Affandi, S.; Green, R. L.; Hsieh, B. T.; Holt, M. S.; Nelson, J. H.; Alyea, E. C. *Synth. React. Inorg., Met.-Org. Chem.* **1987**, *17*, 307–318.

(25) Decken, A. Private Communication 2004, CCDC deposition number 254271.

(26) Nicholson, R. S. *Anal. Chem.* **1965**, *37*, 1351–1355.

(27) See for example: (a) Günes, S.; Neugebauer, H.; Sariciftci, N. S. *Chem. Rev.* **2007**, *107*, 1324–1338. (b) Peet, J.; Kim, J. Y.; Coates, N. E.; Ma, W. L.; Moses, D.; Heeger, A. J.; Bazan, G. C. *Nat. Mater.* **2007**, *6*, 497–500. (c) Park, S. H.; Poy, A.; Beaupré, S.; Cho, S.; Coates, N.; Moon, J. S.; Moses, D.; Leclerc, M.; Lee, K.; Heeger, A. J. *Nat. Photonics* **2009**, *3*, 297–302.

(28) Matano, Y.; Imahori, H. *Org. Biomol. Chem.* **2009**, *7*, 1258–1271.

(29) (a) Norel, L.; Rudolph, M.; Vanthuyne, N.; Williams, J. A. G.; Lescop, C.; Roussel, C.; Autschbach, J.; Crassous, J.; Réau, R. *Angew. Chem., Int. Ed.* **2010**, *49*, 99–102. (b) Hudson, Z. M.; Sun, C.; Helander, M. G.; Amarne, H.; Lu, Z.-H.; Wang, S. *Adv. Funct. Mater.* **2010**, *20*, 3426–2439. (c) Wong, W.-Y.; He, Z.; So, S.-K.; Tong, K.-L.; Lin, Z. *Organometallics* **2005**, *24*, 4079–4082.

(30) Still, B. M.; Kumar, P. G. A.; Aldrich-Wright, J. R.; Price, W. S. *Chem. Soc. Rev.* **2007**, *36*, 665–686.

(31) Rajput, J.; Moss, J. R.; Hutton, A. T.; Hendricks, D. T.; Arendse, C. E.; Imrie, C. *J. Organomet. Chem.* **2004**, *689*, 1553–1568.

(32) Anbalagan, V.; Srinivasan, R.; Pallavi, K. S. *Transition Met. Chem.* **2001**, *26*, 603–607.

(33) Durben, S.; Linder, T.; Baumgartner, T. *New J. Chem.* **2010**, *34*, 1585–1592.

(34) (a) Textor, M.; Ludwig, W. *Helv. Chim. Acta* **1972**, *55*, 184–198. (b) Miskowski, V. M.; Holding, V. H. *Inorg. Chem.* **1989**, *28*, 1529–1533.

(35) (a) Welch, G. C.; Coffin, R.; Peet, J.; Bazan, G. C. *J. Am. Chem. Soc.* **2009**, *131*, 10802–10803. (b) Welch, G. C.; Bazan, G. C. *J. Am. Chem. Soc.* **2011**, *133*, 4632–4644.

(36) Durben, S.; Dienes, Y.; Baumgartner, T. *Org. Lett.* **2006**, *8*, 5893–5896.

(37) Quin, L. D.; Bryson, J. G.; Moreland, C. G. *J. Am. Chem. Soc.* **1969**, *91*, 3308–3316.

(38) Brown, H. C.; Mihm, X. *J. Am. Chem. Soc.* **1955**, *77*, 1723–1726.

(39) (a) Cornforth, J.; Cornforth, R. H.; Gray, R. T. *J. Chem. Soc., Perkin Trans. I* **1982**, 2289–2297. (b) Cornforth, J.; Sierakowski, A. F.; Wallace, T. W. *J. Chem. Soc., Perkin Trans. I* **1982**, 2299–2315. (c) Cornforth, J.; Ridley, D. D.; Sierakowski, A. F.; Uguen, D.; Wallace, T. W.; Hitchcock, P. B. *J. Chem. Soc., Perkin Trans. I* **1982**, 2317–2331. (d) Cornforth, J.; Ridley, D. D.; Sierakowski, A. F.; Uguen, D.; Wallace, T. W. *J. Chem. Soc., Perkin Trans. I* **1982**, 2333–2339.

(40) Zhang, L. H.; Duan, J.; Xu, Y.; Dolbier, W. R., Jr. *Tetrahedron Lett.* **1998**, *39*, 9621–9622.